International Graduate School of Neuroscience

Ruhr University Bochum

Changes in GABAergic mechanisms and cation-chloride co-transports in the albino visual cortex

Doctoral Dissertation

Dmitry Diykov

Thesis advisors: Prof. Dr. Klaus-Peter Hoffmann

PD Dr. Georg Zoidl

Bochum, December 2007

Statement

I certify herewith that the dissertation at hand was completed and written independently and without outside assistance. The "Guidelines for Good Scientific Practice" according to § 9, Sec. 3 were adhered to. This work has never been submitted in this or a similar form at this or any other domestic or foreign institution of higher learning as a dissertation.

Dmitry Diykov

Bochum, 31.12.2007

PhD Commission

Chair:

1st Internal Examiner: Prof. Dr. Klaus-Peter Hoffmann

2nd Internal Examiner: PD Dr. Georg Zoidl

External Examiner:

Non-Specialist:

Date of Final Examination:

PhD Grade Assigned:

TABLE OF CONTENTS

List of figures and tables

List of abbreviations

ACSF	artificial cerebrospinal fluid
AE	anion exchanger
AIDA	(RS)-1-aminoindan-1,5-dicarboxylic acid
AMPA	α-Amino-3-hydroxy-5-methyl-4-isoxazolepropionic acid
CCCs	cation–chloride co-transporters
CPCCOEt	7-(hydroxyimino)cyclopropa-[b]chromen-1a-carboxylate ethyl ester
DHPG	(RS)-3,5-dihydroxyphenylglycine
dLGN	dorsal lateral geniculate nucleus
E_{GABA}	reversal potential of the $GABA_AR$ mediated currents
GABA	γ-aminobutyric acid
$GABA_AR$	$GABA_A$ receptor
KCC2	K^+-Cl^- cotransporter
KYN	kynurenic acid
mGluR	metabotropic glutamate receptor
NDAE	Na.-dependent anion exchanger
NKCC1	Na^+-K^+-$2Cl^-$ cotransporter
NOT-DTN	nucleus of the optic tract and dorsal terminal nucleus
RP	resting potential
trans-ACPD	trans-(6)-1-aminocyclopentanetrans-1,3-dicarboxylic acid
TTX	tetrodotoxin citrate

Abstract

The regulation of intracellular chloride homeostasis plays a crucial role in the maturation of neuronal circuits: while GABA is mostly an inhibitory neurotransmitter in the adult nervous system, it depolarizes cell membranes during development. These actions of GABA rely on differences in the intracellular Cl- concentration: depending on this concentration, Cl- either enters the cell and hyperpolarizes the membrane or leaves the cell and depolarizes it. However, albino visual cortex neurons don't show a corresponding decrease in intracellular chloride concentration during development of the visual system as compared to pigmented animals.

In the first set of experiments (chapter III) I monitored the reversal potential of $GABA_A$ receptor mediated currents during postnatal development in both albino and pigmented visual cortex neurons and showed that after the second week of postnatal development neurons in the visual cortex of albinos start to remain at a more positive reversal potential of $GABA_A$ receptor mediated currents than neurons from the same brain area in pigmented animals. This finding supports the hypothesis of an aberrant maturation of albino visual circuits rather than the existence of inborn abnormalities.

In the second set of experiments (chapter IV) we monitored expression of two major chloride regulators in neocortical neurons on a single cell level: the Na^+-K^+-$2Cl^-$ co-transporter (NKCC1, Cl^--uptake) and the K^+-Cl^- co-transporter (KCC2, Cl^--extrusion) in albino and pigmented rat visual cortex neurons coupled with gramicidin perforated patch clamp analysis. We revealed a qualitative difference in NKCC1, but not KCC2 mRNA expression between albino and pigmented rat visual cortex neurons. Pharmacological blockade of NKCC1 function with its specific

inhibitor, bumetanide, during electrophysiological recordings and subsequent single cell real time PCR analysis of the co-transporter mRNA linked the inhibitory deficit observed in albino visual cortical network almost exclusively to the high expression of NKCC1.

In chapter V we discuss the impact of mGluR antagonist to the reversal potential of GABAA receptor mediated currents. We revealed a significant shift of E_{GABA} towards hyperpolarization by block of metabotropic glutamate receptors in albinos, but not in pigmented animals. These data are discussed in regard to known effects of metabotropic glutamate receptor (mGluR) agonists.

Taken together our results suggest that NKCC1 may be the leading cause of the observed elevated intracellular chloride level in albino visual cortex neurons. I propose a model of regulation of the most important chloride regulator responsible for chloride uptake - Na^+-K^+-$2Cl^-$ co-transporter in albino visual cortex neurons.

Chapter I

Introduction

Albinism is a disorder of amino acid metabolism that results in a congenital hypopigmentation of ocular and systemic tissues. Tyrosinase-positive and -negative oculocutaneous albinos possess an autosomal recessive inheritance pattern. Oculocutaneous albinism results from incomplete melanization of the cellular melanosomes. In tyrosinase-negative oculocutaneous albinism, the congenital inactivity of the enzyme tyrosinase prevents the cell's use of tyrosine in the formation of the pigment melanin. In tyrosinase-positive oculocutaneous albinism, tyrosinase activity is normal, but there is an inability of the cells to sequester the synthesized melanin into the melanosomes.

Ocular albinism, in contrast to oculocutaneous albinism, exhibits pigmentary dilution due to abnormalities in melanosome synthesis rather than inadequate melanization. Ocular albinism is transmitted through either an X-linked or autosomal recessive mode. The hair and skin of the ocular albino tends to show a much greater pigmentation than that of the oculocutaneous albino, often falling into a normal pigmentation range. The uveal pigmentation of the ocular albino is variable and may range from very hypopigmented to a nearly normal pigmentation level.

Tyrosinase produces the cascade of reactions that ultimately results in the production of melanin in the skin and the eyes, but it does not produce melanin in other regions of the CNS, such as the substantia nigra. The catalytic enzyme involved in melanin production is tyrosine hydroxylase. Tyrosinase catalyses the reaction between tyrosine and dopa, and between dopa and dopaquinone which are early stages in melanin synthesis (Fig. 1.1) (Kinnear et al. 1985). Each of the deficits associated with albinism has been corrected by the introduction of a functional *tyrosinase* gene in transgenic mice and rabbits (Jeffery et al. 1994; 1997).

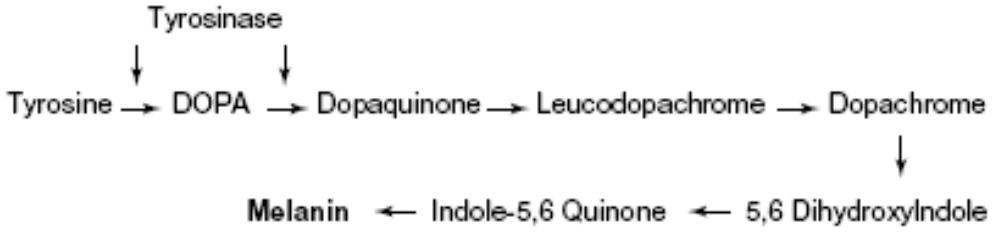

Fig.1.1: A simplified schematic representation of the synthetic pathway of melanin. In many forms of albinism, tyrosinase, which catalyses the reaction between tyrosine and dopa and between dopa and dopaquinone, is absent (from Jeffery 1997).

The normal projection of visual fibers from the retina is severely disrupted in albinism, where the line of decussation is shifted into the temporal retina, such that a far greater number of fibers from temporal

retina cross the midline and project contralaterally than in the normal (Lund, 1965; Creel, 1971; Guillery and Kaas, 1973; Creel et al., 1974; Guillery et al., 1975; Apkarian et al., 1983; Guillery, 1986; Hedera et al., 1994; Jeffery, 1997; Morland et al., 2001, 2002).

		Pattern			Method		
Animal	Study	B	M	A	E	H	B
Cat							
Siamese	Hubel and Wiesel, 1971	5/7	2/7		x		
Siamese	Kaas and Guillery, 1973	1/12	11/12			x	
Siamese				13/13	x		
Siamese	Elekessy et al., 1973		6/6				x
Siamese	Guillery et al., 1974		3/3				x
Siamese	Guillery and Casagrande, 1977		1/1		x		
Siamese		1/9	8/9			x	
Siamese	Shatz, 1977	11/12	1/12		x		
Siamese	Montero and Guillery, 1978		4/4		x		
Siamese	Shatz and LeVay, 1979	6/6				x	
Siamese	Chino et al., 1980		12/12		x		
Siamese	Cooper and Blasdel, 1980[a]	4/4	4/4		x		
Siamese	Antonini et al., 1981	9/9			x		
Siamese	Toyama et al., 1991	9/9			x		
Siamese	Berman and Grant, 1992	6/6			x		
Siamese	Ault et al., 1995	1/1					
hz Albino		1/1					
Albino	Leventhal and Creel, 1985		44% S	56% S	x		
				3/3 X	x		
Albino	Schmolesky et al., 2000		2/2 S	2/2 X	x		
hz Albinism	Leventhal et al., 1985	5/5 X	5/5 S		x		
Mink							
Hypopimented	Guillery et al., 1979	3/18	15/18			x	
Ferret							
Albino	Huang and Guillery, 1985	4/8	4/8			x	
Albino	Ackerman et al., 2003[b]	22/25	3/25		x		
		11/14	3/14			x	
Albino	Garipis and Hoffmann, 2003		5/5				x
Monkey							
Albino	Guillery et al., 1984			1/1	x		

Table 1.1: Summary of previous reports on the cortical organization pattern in animal models of albinism (taken from Hoffmann et al. 2003)

Cortical patterns: B, Boston; M, Midwestern; A, true albino. Cortical area (S, striate; X, extrastriate) is indicated if study reports differential organization in different cortical areas. Method: E, single cell electrophysiology; H, histology (HRP, retrograde degeneration, 3H-Proline, fluorescent beads); B, behavior; hz, heterozogous for albinism.

*a*Boston and Midwestern patterns were dominant in the lower visual field and along the horizontal meridian, respectively.

*b*Boston and Midwestern patterns were dominant in the upper and lower visual field, respectively. The values of 22/25 and 11/14 are the lower limits of the estimated prevalence of the Boston pattern, because the upper hemifields were not tested in each of the animals.

n - number of individuals with a given pattern; *m* number of individuals studied.

There are three cortical projection patterns, associated with albinism: “true-albino”, “Midwestern” and “Boston”.

(1) Even if the rerouting at the chiasm does not affect the geniculocortical projection, the visuotopic map in albinos will be extremely abnormal: contralateral and ipsilateral hemifields will have a strong representation in the same part of visual cortex. This projection pattern is regarded as “true-albino”. It has been found in tyrosinase-negative albino cats (Leventhal and Creel, 1985; Schmolesky et al. 2000), albino monkey (Guillery et al., 1984), and albino people (Hoffmann et al. 2003).

(2) Representation of the ipsilateral hemifield may be relatively weaker in cortex than in dorsal lateral geniculate nucleus (dLGN); it indicates some cortical suppression. If the geniculocortical projection is anatomically normal, but there is no evidence for any functional input

from the misrouted contralateral temporal retina, (cortical suppression of the abnormal input is complete) then it is a case of “Midwestern” pattern. It has been found in most of the Siamese cats studied by Kaas and Guillery (1973) and in albino cats studied by Schmolesky et al. (2000); they conclude that the suppression of abnormal dLGN cell inputs, abnormal cortical cell activity, or both, may underlay reduced numbers of visually driven abnormal cells in cortex relative to the dLGN. Some human albinos also show reduced sensitivity to stimuli obtained by the temporal hemiretina, but not the nasal hemiretina (St John and Timney, 1981). As a consequence each hemisphere responds rather to stimuli delivered to one visual field and not the another, similar to cortical function in normal animals. So, “Midwestern” pattern looks like the mapping in normal pigmented mammals. This resemblance occurs because the input from the ipsilateral field is physiologically suppressed in cortex.

(3) If there is clear functional input from both temporal and nasal contralateral retina in striate cortex, then it is called “Boston” pattern. Geniculocortical projections are reorganized to generate a permanent and consistent mapping of the ipsilateral visual field into each hemisphere The representation of the vertical midline is no longer at the 17/18 border but is displaced well inside area 17 (Akerman et al. 2003).

It has been found in most of the Siamese cats recorded by Hubel and Wiesel (1971) and albino ferrets recorded by Akerman et al. (2003). To form the “Boston” mapping, there must be an additional alteration in the targeting of geniculate axons (Akerman et al. 2003).

Although the presence of these diverse cortical projection patterns in the albino visual cortex is well-known, the factors underlying their genesis are still unclear. The “Boston” pattern appearing, probably, if the representation of the vertical meridian is displaced by only 1–2 mm (Akerman et al. 2003). It was seen in “Boston” Siamese cats (Hubel and Wiesel, 1971; Kaas and Guillery, 1973; Shatz, 1977; Cooper and Blasdel, 1980) and “Boston” albino ferrets (Akerman et. all 2003). These data may represent the highest possibility of cortical reorganization.

In normal people decussation of the optic fibres is loyal to the vertical meridian that passes through the fovea: fibres from the temporal retina project ipsilaterally to the lateral geniculate nucleus and cortex, whereas fibres from the nasal retina project contralaterally. In albinos, however, a higher than normal proportion of fibres from the temporal retina project contralaterally. The line of decussation is, therefore, shifted to the peripheral ipsilateral visual field. Finally line of the decussation in the human was detailed as a vertical meridian that is shifted into the

temporal retina (Hoffmann et al. 2003). This abnormal projection of a part of the temporal retina to the visual cortex, together with the normally routed fibres from nasal retina, provides a cortical hemisphere with visual input from more than the normal hemifield of visual space. Due to predominantly monocular innervations of the left and right hemispheres, the unilateral activation of the visual cortex (lateralisation) can be detected with visual evoked potentials. It was found with multichannel pattern onset visual evoked potentials that pathological crossing of the nerve fibres in the optic chiasm is always detectable in oculocutaneous and ocular albinism, but had never been detected in normal humans (Torok, 2001; Kasmann-Kellner et al. 2003). Thus, lateralisation of visual evoked potentials appeared to be a better indicator of ocular albinism than other symptoms as macular hypoplasia, hypopigmentation, iris transillumination, nystagmus, reduced visual acuity and so on. But due to the restricted spatial resolution (Morland et al. 2002), visual evoked potentials analyses cannot answer questions of albino cortical organisation such as the representation of the visual field in the early visual areas and the degree of cortical magnification.

Human albinos show congenital nystagmus without oscillopsia. Consequences of atypical chiasmatic crossing were demonstrated with monocular visual stimulation using functional magnetic resonance

imaging (fMRI) (Schmitz et al. 2004). They observed contralaterally dominated activation of visual cortices correlating to clinical albinism parameters. This confirms albinism as a continuous range of hypopigmentation disorders. Additionally, albinos showed activation of the superior colliculus and of visual motion areas although the stimulus was stationary.

Albino misrouting (Apkarian, 1992; Kriss et al. 1992; Morland et al. 2002; Schmitz et al. 2004) is shown clearly during an independent visual stimulation of both hemifields: activity in the occipital cortex in the normal humans is contralateral to the stimulated visual field, whereas it is contralateral to the stimulated eye in the albino, independent of the stimulated visual field (Morland et. al. 2002). Thus, the albino visual cortex is activated not only by stimulation in the contralateral visual field, but also by abnormal input from the ipsilateral visual field.

There are conflicting reports on cortical activity ipsilateral to the stimulated eye. Morland et al. (2002), stated that fMRI data directly showed that in the albino it is indeed the occipital lobe contralateral to the stimulated eye that is active during stimulation in each hemifield, whereas the control subject hemispheres were only active during stimulation in the contralateral visual field. Activity ipsilateral to the

stimulated eye was strongly reduced in the albino. Hedera et al. (1994) documented some cortical activity ipsilateral to the stimulated eye: substantial residual ipsilateral activity in the more anterior portion of the fundus of the calcarine sulcus.

Input from temporal retina is not substantially suppressed in humans and forms a retinotopic mapping that is superimposed on the mapping of the nasal retina in striate and extrastriate areas. The abnormal routing of temporal fibres is not total, with the line of decussation shifting to between 6 and 14° into temporal retina (Hoffmann et al. 2003). Input to visual cortex in human albinism does not undergo topographic reorganization between the thalamus and cortex and, moreover, is not significantly suppressed in either striate or extrastriate areas. Nasal and temporal retinas have their visuotopic representations superimposed in early extrastriate areas. Thus, one may conclude that cells in striate and extrastriate areas that normally respond to binocular input would not develop to act in response to input from binocularly corresponding retinal locations. Topographic mapping in humans does not match to the normally observed patterns in other mammals but takes the form of the "true albino" pattern. This mapping is consistent with that documented in the only other primate studied (Guillery et al. 1984). On one hand it would appear, therefore, those developmental mechanisms that allow

the thalamocortical projections to be reorganized in some mammals are not available to the primate. On another hand, abnormal projection of the temporal retina was observed predominantly in the central part of the visual field (Hoffmann et al. 2003). Hence, the fundamental origin of the albino abnormality appears to be expressed in the same way in primates as in other species.

Albino mammals often are unable to perform regular optokinetic eye movements to stabilize the visual environment (for a recent review see Hoffmann et al., 2004). In rats and ferrets this optokinetic defect could be directly linked to a loss of direction selectivity in the nucleus of the optic tract and dorsal terminal nucleus (NOT-DTN), the sensorimotor interface in the pathway subserving the optokinetic reflex (Lannou et al., 1982; Hoffmann et al., 2004). As direction selectivity in the NOT-DTN arises from direction selective retinal ganglion cells (turtle: Rosenberg & Ariel, 1991; rabbit: Oyster *et al*., 1972; cat: Hoffmann & Stone, 1985) and from direction selective pyramidal cells in motion sensitive cortical areas (cat: Schoppmann 1985; monkey: Hoffmann *et al*., 2002) one can hypothesize that direction selectivity must be generally disturbed in the visual system of albino mammals. There is growing evidence that direction selectivity in the retina and visual cortex critically depends on GABAergic mechanisms and cation-chloride cotransporters (e.g. Kittila

& Massey, 1997; Taylor et al. 2000; Gavrikov et al. 2003; Thiele et al. 2004).

One classical type of GABAergic transmission emerges in a way that, following depolarization of the presynaptic terminal, GABA is briefly released from transmitter vesicles and binds to postsynaptic GABAA receptors. In the CNS, the cation–chloride co-transporters (CCCs) play a key role in intracellular Cl- regulation (Kaila 1994). In order for Cl- to mediate currents across the resting membrane through GABA- or glycine-gated anion channels, intracellular Cl- must be maintained afar from electrochemical equilibrium. Cl- transport mediated by CCCs is performed without any net charge movement across the membrane (i.e. the CCCs are electroneutral) and the transport cycles are driven without the direct hydrolysis of ATP (i.e. the CCCs are secondarily active). The energy for net transport is mainly derived from the cation gradients generated by the Na./K.-ATPase. Other secondarily active transport proteins can also participate in overall neuronal Cl- homeostasis, including Na.-dependent and Na independent anion exchangers (NDAE and AE, respectively), which exchange Cl- for HCO_3- (Grichtchenko et al. 2001; Romero et al. 2000). Secondarily active Cl- transporters and their basic modes of operation are presented in fig. 1.2.

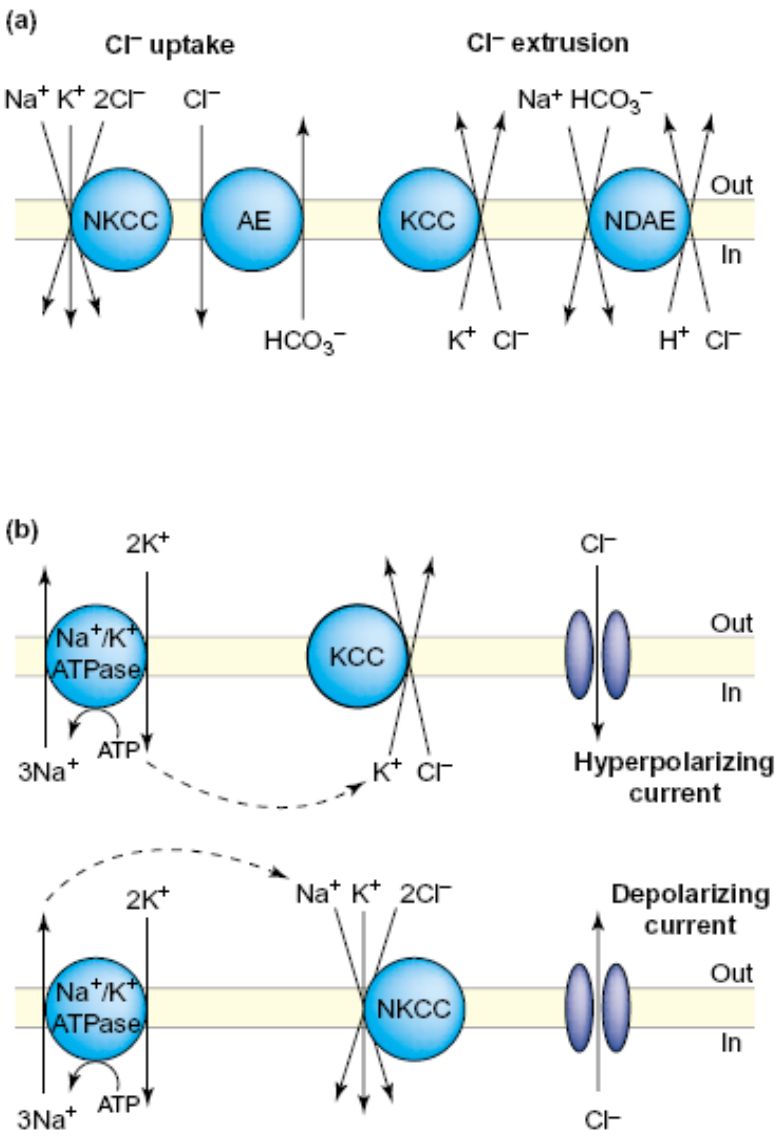

Fig.1.2: Secondarily active Cl- transporters and their basic modes of operation.(a) Under physiological conditions, Cl- uptake is mediated by Na–K–2Cl co-transporters (NKCCs) and Na.-independent anion exchangers (AEs), whereas K–Cl co-transporters (KCCs) and Na.-dependent anion exchangers (NDAEs) extrude Cl2. As HCO_3- is a substrate for AEs and NDAEs, these two transporters are also directly involved in the regulation of intracellular pH. Arrows indicate the direction of net transport. (b) The transport of Cl- by secondarily active transporters is driven by the

concentration gradients of cations. The K. gradient generated by the Na./K.-ATPase fuels the extrusion of Cl- by KCC, which results in an inwardly directed electrochemical gradient for Cl- that generates hyperpolarizing currents across anion-permeable channels (top). Uptake of Cl- by NKCCs (bottom) is driven mainly by the energy taken from the Na. gradient, and the resulting outwardly directed Cl- electrochemical gradient permits depolarizing Cl- currents. (source: Payne et al. 2003)

The CCC gene family consists of three broad groups (Fig. 1.3): Na–Cl co-transporters (NCCs), Na–K–2Cl co-transporters (NKCCs) and K–Cl co-transporters (KCCs). Under normal physiological conditions, NCC and NKCC function in active Cl- accumulation, whereas KCC operates in active Cl- extrusion. As electroneutral transporters they are bi-directional pumping Cl- in or out, depending on the concentration gradients of the transported ion. NCC has not been found in nervous tissue (Gamba et al. 1994). The developmental switch to an inhibitory action of GABA is a consequence of a decrease of NKCC1 and increase of KCC2 expression (Payne et al. 2003; Yamada et al. 2004; Stein & Nicoll 2003; Sung et al. 2000). During development, net active chloride transport is inward, so that anions flow out of the neuron when the GABAA channel is opened. This depolarizes the membrane strongly enough to activate voltage-dependent calcium channels (Owens et al.

1996) and relieve the Mg2+ block of the NMDA receptor (Ganguly et al. 2001). The resultant calcium transients have important effects on the growth and development of the neuron, but as excitatory glutamatergic synapses become more plentiful, GABA needs to become inhibitory in a hurry to stabilize the new neural networks (Staley & Smith, 2001). A binding site for neuronal-restrictive silencing factor was recently discovered on the KCC2 gene (Karadsheh & Delpire, 2001); it is possible that the calcium transients trigger the life-long increase in KCC2 by initiating the events that remove this negative control of KCC2 expression. The chain of events that change the effect of GABAA receptor activation from excitation to inhibition is presented in fig. 1.4.

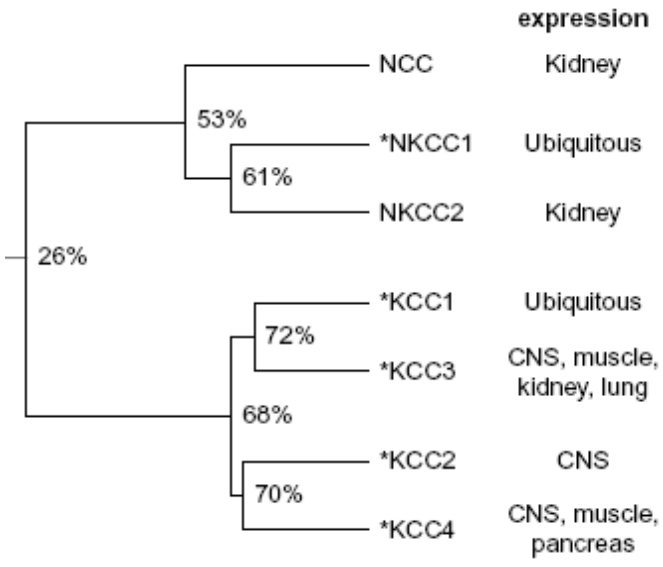

Fig. 1.3: Phylogenetic tree of human cation–chloride co-transporters (CCCs). The percentage of identical residues between aligned protein sequences is shown at branch points. (source: Payne et al. 2003)

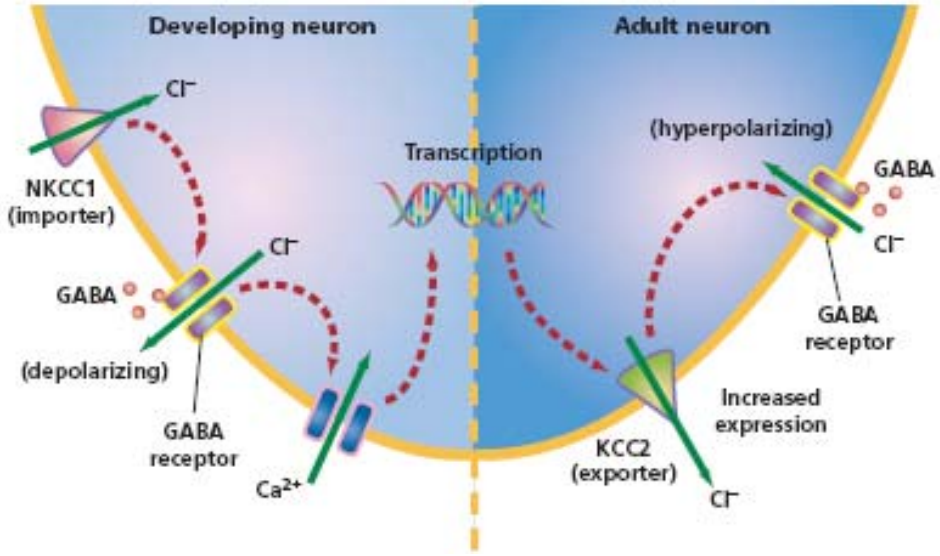

Fig 1.4: GABAA receptor activation is the newest link in the chain of events that change the effect of GABAA receptor activation from excitation to inhibition. Electroneutral Cl– transport is reversed in adult versus developing neurons because of the increased expression of KCC2 in adults (source: Staley & Smith, 2001).

Chapter II

Aims of the study

Albino mutations lead to a loss of direction selectivity in the motion sensitive cortical areas of albino mammals. This, in turn critically depends on GABAergic mechanisms. While GABA is the main

inhibitory transmitter in the adult brain GABAergic transmission is excitatory during early postnatal development. The different action of GABA results from a reversed chloride concentration gradient with higher intracellular chloride concentration in immature neurons. The Na^+-K^+-$2Cl^-$ co-transporter (NKCC1, Cl^--uptake) and the K^+-Cl^- co-transporter (KCC2, Cl^--extrusion) are the most important of the many known chloride regulators in neocortical neurons. The developmental switch to an inhibitory action of GABA is a consequence of a decrease of NKCC1 and increase of KCC2 expression.

However, little is known about the effect of albinism on these mechanisms. It is known that neurons in the adult albino Wistar rat visual cortex have shifted their reversal potential of $GABA_AR$ mediated currents (E_{GABA}) in the depolarizing direction when compared to pigmented Long Evans rats, but postnatal development of GABAergic transmission in albino visual cortex and its molecular basis remained unknown so far. Therefore, primary goals of my thesis were:

- First, to describe the postnatal development of inhibitory postsynaptic currents in albino visual cortex
- Second, to evaluate the impact of changed GABAergic transmission for networks in the albino visual cortex.

- Third, to detect molecular mechanisms underlying elevated intracellular chloride concentration and its consequence the shift of E_{GABA} in the depolarizing direction in albino visual cortex neurons.

Chapter III

Postnatal development of the reversal potential of the $GABA_A$ receptor mediated currents (E_{GABA}) in albino visual cortex neurons

Abstract

Albinism has a profound effect on visual development and visual function. Significant alterations of GABAergic mechanisms were found in P28-35 albino rat visual cortex neurons, comprising shifted reversal potential of the $GABA_AR$ mediated currents (E_{GABA}) to more positive values in albinos in comparison to pigmented animals. In this study we compare early postnatal development of E_{GABA} in visual cortex neurons of albino and pigmented rats. At birth we found no differences. At the time of eye opening (second week postnatally) the reversal potential of $GABA_AR$ mediated currents is 15mV more positive and intracellular Cl^- concentration is higher in visual cortex neurons of albinos than of pigmented rats. Functional analysis of this phenomenon indicates that albino visual cortex networks show reduced possibility for neuronal coding and explains existing hyperexcitability in albino visual cortex neurons.

Motivation

The change of GABA and glycine mediated responses from depolarizing to hyperpolarizing reveals a change in the driving force for Cl^- and a shift in GABA and glycine reversal potential during development (Ben-Ari, 2002; Payne et al. 2003; Rivera et al. 1999; Yamada et al. 2004). It has been shown recently that neurons in the adult albino Wistar rat visual cortex have changed $GABA_AR$ mediated currents in comparison to pigmented Long Evans neurons (Barmashenko et al. 2005). This finding, however, has opened several questions. First, it was unclear whether a similar difference is already present at birth or appears during postnatal development of the visual system. Second, as this study was performed on different rat strains, it opened the possibility that strain variations can contribute to the observed differences. Third, functional impact of this phenomenon on visual cortex networks in albinos had to be determined. To address these questions we investigated the early postnatal development of chloride homeostasis in visual cortex of pigmented Long-Evans and albino Wistar rats as well as in pigmented and albino littermates.

Materials and methods

Animals

Experiments were carried out on Long-Evans and Wistar rats of postnatal day (P) 1-40 and second generation of homozygous and heterozygous animals obtained by cross breeding the rat strains. For detailed method see (Ilia & Jeffery, 2000). All experimental procedures were approved by the local ethics committee and were performed in accordance with the European communities Council directive of 24 November 1986 (S6 609 EEC) and National Institutes of Health guidelines for care und use of animals for experimental procedures.

Brain slice preparation

Rat pups were anesthetized with halothane and decapitated. The brain was taken out of the skull and immersed in ice-cold artificial cerebrospinal fluid (ACSF; 123 mM NaCl, 2.5 mM KCl, 1 mM NaH_2PO_4, 26 mM $NaHCO_3$, 11 mM D-glucose, 1.8 mM $CaCl_2$, 1.3 mM $MgCl_2$, bubbled with 95% O_2 and 5% CO_2, pH 7.4). Slices of visual cortex (350µm) were cut on a vibratome (MA752, Campden Instruments, Germany). In the P40 animals the slices were derived from Bregma –5.8mm to Bregma –7.5mm (Paxinos et al. 1985), where the visual cortical areas 18, 17 and 18a extend 7-8mm from the midline

laterally to the temporal cortex. Slices were stored for at least 1 h at room temperature in ACSF and then relocated to a submerged recording chamber.

Gramicidin-perforated patch-clamp recordings

The techniques we used for perforated patch clamp recording have been reported in detail elsewhere (Barmashenko et al. 2005). The recording chamber was perfused with oxygenated ACSF at room temperature at a rate of 3 ml/min. Kynurenic acid (2 mM) was added directly to the ACSF to prevent excitatory activity in the neurons tested. Gramicidin perforated patch clamp recordings of pyramidal neurons were performed under visual control (fig 3.1). All recorded cells were from layer V or pyramidal neurons in cortical plate (P1-3). Borosilicate patch electrodes (5-9 MΩ) were filled with a solution containing 130 mM K-gluconate, 0.5 mM Na-gluconate, 20 mM HEPES, 4 mM MgCl2, 4 mM Na2ATP, 0.4 mM Na3GTP, 0.5 mM EGTA (pH 7.2). Gramicidin (30 μg/ml, dissolved in DMSO, Sigma) was added to the solution as a membrane perforating agent. The measured membrane potentials were corrected for the junction potential of -10 mV (Mienville & Pesold, 1999). Inhibitory postsynaptic currents (IPSCs) were evoked through a concentric bipolar electrode placed approximately 50-100 μm lateral to

the recorded neuron with stimuli (20-100 μA, 50 μs duration, 0.1 Hz) in voltage clamp mode by means of a PC-501A patch clamp amplifier (Warner Institute Corporation) connected via AD/DA-converters (CED 1401+, Cambridge Electronic Design, UK) to a personal computer(fig 3.2). Holding potentials were raised from -100 to +30 mV (keeping in mind the junction potential correction of -10 mV) in 10 mV steps in every recording. Recordings underwent low-pass filtering at 3 kHz and were sampled at 10 kHz.

Calculation of intracellular chloride concentration

Equilibrium potential for each ion is determined solely by the concentration gradient and valence, by the Nernst equation:

$$V_{\text{Eq.}} = \frac{RT}{zF} \ln\left(\frac{[X]_{\text{out}}}{[X]_{\text{in}}}\right)$$

where:

- $\boldsymbol{V_{\text{Eq.}}}$ is the equilibrium (measurable) reversible potential for a given ion, in our study it is Cl- ion.
- ***R*** is the universal gas constant (8.314 $J.K^{-1}.mol^{-1}$).
- ***T*** is the temperature in Kelvin (°K = °C + 273.15).

- ***z*** is the valence of the ionic species.
- ***F*** is the Faraday's constant (96485 $C.mol^{-1}$).
- $\mathbf{[}X\mathbf{]_{out}}$ is the concentration of the ionic species *X* in the extracellular fluid (Cl^{1-}).
- $\mathbf{[}X\mathbf{]_{in}}$ is the concentration of the ionic species *X* in the intracellular fluid (Cl^{1-}).

Drugs

The drugs applied were gramicidin D, kynurenic acid (KYN, an ionotropic glutamatergic receptor antagonist), bicuculline (an ionotropic GABAA receptor antagonist) and picrotoxin citrate (an ionotropic GABA receptor antagonist) (Tocris Cookson, Bristol, UK). Substances were prepared as stock solutions and frozen, then added to the ACSF to reach the desired final concentration.

Data acquisition and calculating

For recording and analyzing WinWCP software (John Dempster, University of Strathclyde, Glasgow, UK) was used. One way ANOVA ($p < 0.001$), SigmaStat 2.03 software, was used to test the data for significant disparities. Numerical data are presented as mean ± S.D.

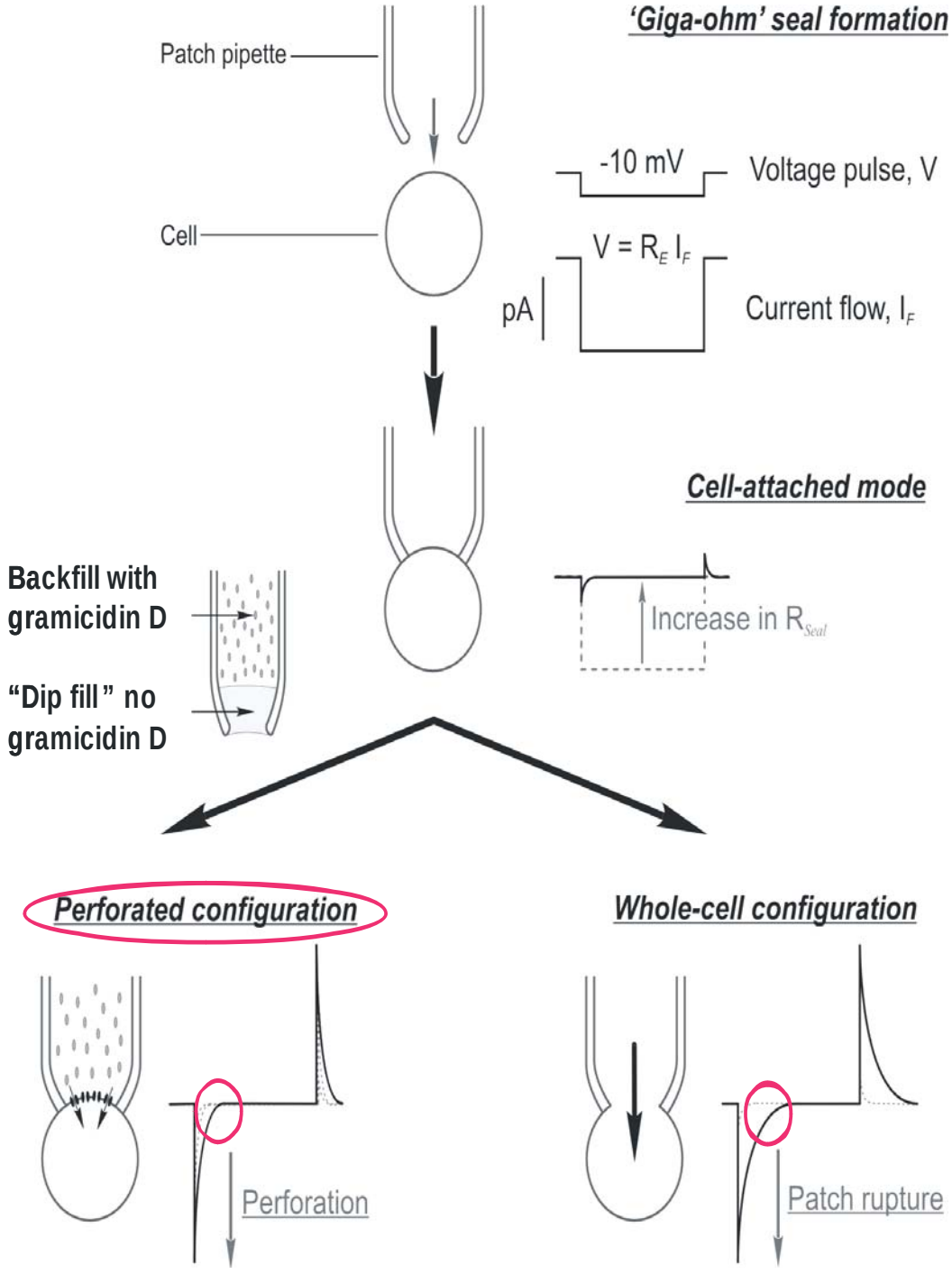

Fig 3.1: Schematic of gramicidin perforated patch clamp recordings

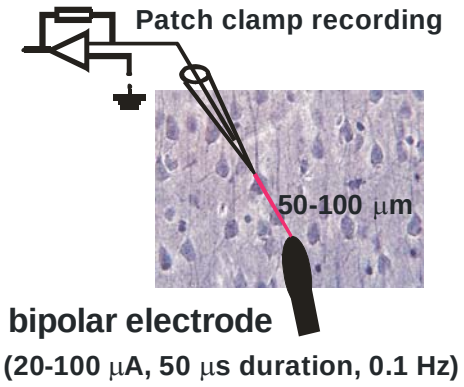

Fig 3.2: Lateral stimulation of the recorded neuron in voltage clamp mode

Results

Visual cortex neuronal $GABA_A$ receptor mediated currents were measured at different holding potentials and E_{GABA} was determined from these recordings. In order to investigate the development of inhibitory pattern in albino visual cortex neurons, recordings were taken from 4 different age groups of albino Wister rats: P1-5, P7-9, P14-17 and P>20. Recordings from visual cortex of pigmented Long Evans rats of the same age groups were taken as a control. Data are presented in figure 3.3a. Intracellular chloride levels for the above mentioned groups were calculated from $GABA_AR$ mediated currents reversal potential according to the Nernst equation (T=25^oC) and comprised 29,15 versus 28,09; 20,61 versus 16,34; 21,07 versus 11,47 and 19,73 versus 11,03 mM for albino and pigmented visual cortex neurons respectively (fig.3.3b). By application of the $GABA_AR$ antagonist bicuculline (30 μM) and GABAAR antagonist picrotoxin (1 μM) all PSCs disappeared.

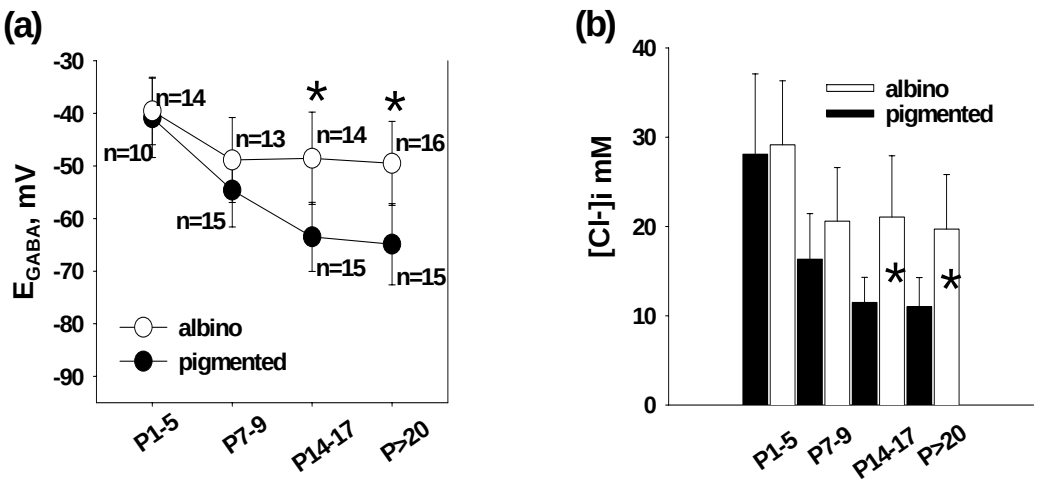

Fig 3.3: **(a)** Postnatal development of $GABA_AR$ mediated currents reversal potential (E_{GABA}) in visual cortex neurons of albino and pigmented rats. **(b)** Estimation of intracellular chloride concentration ($[Cl^-]_i$) in visual cortex neurons of albino and pigmented rats, T=25^{o}C. Data are presented as mean ±S.D (*p<0,001, Mann-Whitney rank sum test). Axes: x(a and b) – age groups, P – postnatal days; y(a) – reversal potential of GABAA receptor mediated currents, mV, y(b) – intracellular chloride concentration($[Cl^-]_i$), mM.

To exclude strain variations we compared the properties of P20-40 visual cortical neurons of the parental and the second generation of homozygous albino and homozygous and heterozygous pigmented littermates. We examined E_{GABA} and resting potentials and calculated the intracellular chloride concentration for the above mentioned groups. No statistically significant contribution of strain variations to altered

$GABA_AR$ mediated currents in albino visual cortex neurons was found. E_{GABA} in visual cortical neurons of parental and second generation rats was -65,75 and -67,75 and -50,95 and -49,95 mV for pigmented and albino animals respectively (fig 3.4a). Resting potentials of these groups were -70,30 and -69,29 and -65,54 and -63,55 mV (fig 3.4b). Calculated values of intracellular chloride presented in fig.3.4c were 11,22 and 10,63 mM in pigmented and 20,23 and 21,03 mM in albino rats.

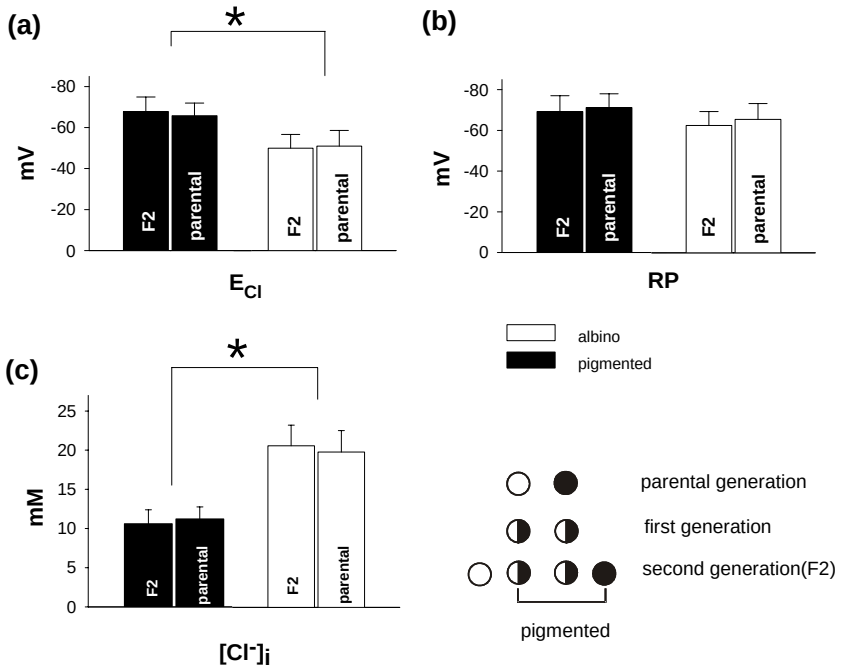

Fig 3.4. (a) and **(b)** Comparison of E_{GABA} and resting potential (RP) (mV) in visual cortical neurons between parental and the second generation (F2) of homozygous albino and heterozygous and homozygous pigmented animals, P>15. **(c)**

Corresponding estimation of intracellular chloride concentration ($[Cl^-]_i$), (mM). T=25^oC. Data are presented as mean ±S.D ($^*p<0,001$, one way ANOVA).

Unblocked condition

In order to evaluate the impact of elevated intracellular chloride levels in albino visual cortex neurons on cortical networks we conducted gramicidin perforated patch clamp analysis of both albino and pigmented layer V visual cortex neurons without blocking of excitation during physiological recordings. We found that the reversal potential of postsynaptic currents (combined inhibitory and excitatory) significantly differ between albino and pigmented animals, being shifted to depolarizing direction in albinos (-49,2+/-1,35mV, n=16 in albino vs. -58,23+/-2,31mV, n=10; in pigmented animals fig 3.5). One should keep in mind that the observed difference may result from variable inhibitory and/or excitatory inputs to characterized cells. Thresholds for action potentials (AP) were not significantly different between the two experimental groups and comprised -38,14+/-1,69 (n=10) for pigmented and -43,50+/-2,02 for albino (n=16) (fig 3.6), but the difference between resting membrane potential and the AP threshold was statistically significant: 33,6+/-2,65mV(n=10) for pigmented neurons vs. 19,49+/-3,05mV (n=16) for albino neurons (fig 3.7). These findings may be explained as hyperexcitability in albino visual networks: neurons in

albino visual cortex need less depolarization in order to reach AP threshold. Surprisingly, minimal interspike intervals were significantly longer in albinos than in pigmented (fig 3.8): 28,16+/-2,92ms(n=16) vs. 23,23+/-2,62ms(n=10). Oscillations within and across neuronal systems are believed to serve various complex functions, such as perception, cognition, movement initiation, plasticity and memory. GABAergic interneurons and their inhibitory synapses play a major role in these oscillatory patterns. Networks of inhibitory interneurons impose a coordinated oscillatory "context" for the "content" carried by networks of principal cells (Buzsaki, 2001). This hypothesis implies that GABAergic neuronal networks may cooperatively entrain large populations of pyramidal cells throughout the neocortex (for reviews see Wang et al. 2006; Mazzoni et al. 2007). Therefore, the increase in minimal interspike intervals in albino neuron may indicate a reduced possibility for high frequency neuronal coding in albino visual cortex networks.

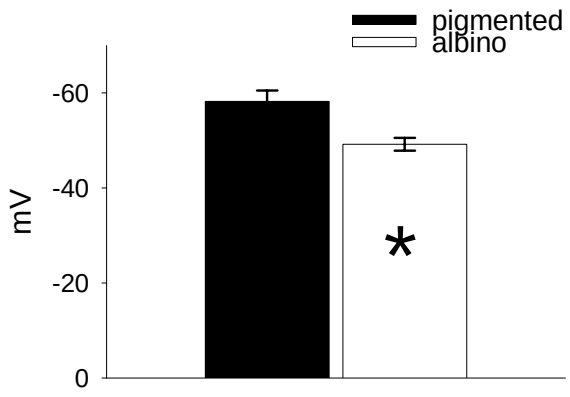

Fig 3.5: Reversal potentials of postsynaptic currents (mV) in visual cortical neurons of albino and pigmented animals (excitation wasn't blocked during physiological recordings). Data are presented as mean ±S.D (*p<0,001, one way ANOVA).

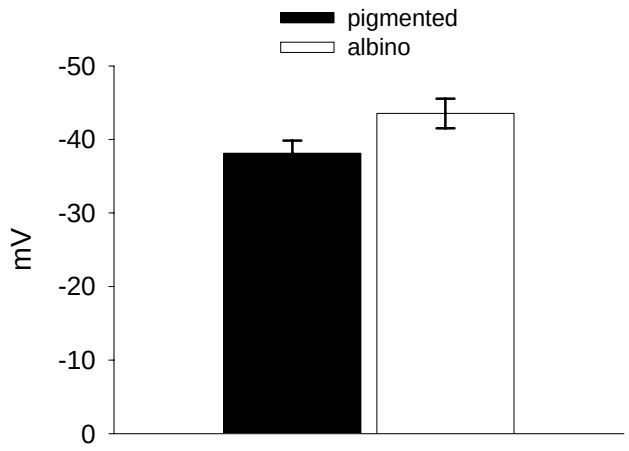

Fig 3.6: Thresholds for action potentials in albinos and pigmented visual cortex neurons (mV). Data are presented as mean ±S.D (p>0,05, one way ANOVA).

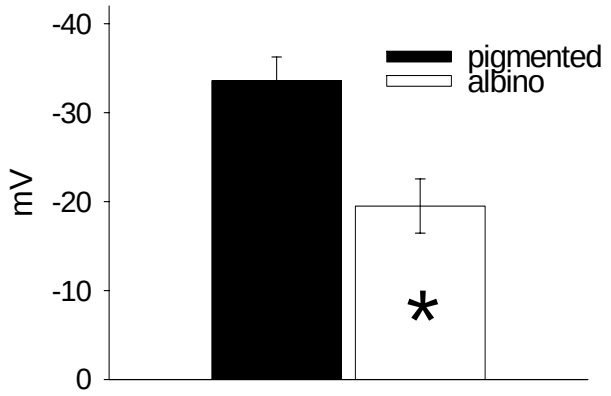

Fig 3.7: Differences between resting membrane potential and action potential thresholds (mV) in albino and pigmented rat visual cortex neurons. Data are presented as mean ±S.D (*p<0,001, one way ANOVA).

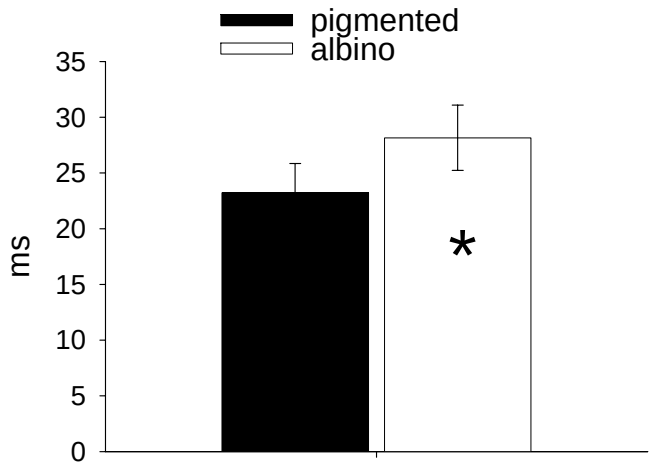

Fig 3.8: Minimal interspike intervals (ms) in albino and in pigmented visual cortex neurons elicited by applying depolarizing current steps (current clamp mode, steps are 200 ms duration). Data are presented as mean ±S.D (*p<0,001, one way ANOVA).

Discussion

The regulation of intracellular chloride homeostasis plays a crucial role in the maturation of neuronal circuits: while GABA is mostly an inhibitory neurotransmitter in the adult nervous system, it depolarizes cell membranes during development. These actions of GABA rely on differences in the intracellular Cl^- concentration: depending on this concentration, Cl^- either enters the cell and hyperpolarizes the membrane or leaves the cell and depolarizes it (Delpire 2000). Owens et al. in 1996, using the perforated patch clamp technique showed a decrease in neuronal Cl^- concentration during postnatal development in GABAergic neurons from the neocortex. The same pattern was reported for glycinergic neurons from the auditory brain stem (Ehrlich et al. 1999).

The present study describes and compares the postnatal development of inhibitory postsynaptic currents of pyramidal neurons in slices of visual cortex from pigmented and albino rats. We monitored the reversal potential of $GABA_A$ receptor mediated currents during postnatal development in both albino and pigmented visual cortex neurons and showed that after the second week of postnatal development neurons in the visual cortex of albinos start to remain at a more positive reversal

potential of $GABA_A$ receptor mediated currents when compared to pigmented animals. This finding supports the hypothesis of an aberrant maturation of albino visual circuits rather than the existence of inborn abnormalities. Interestingly, the calculated intracellular chloride concentration in albino visual cortex neurons exceeded almost twice that in pigmented animals after postnatal day 14 (19,73 versus 11,03mM respectively), a fact that confirms the recent findings published by Barmashenko et al. in 2005. In that paper, using furosemide and bumetanide as blocking agents of the two most important chloride-transporters - KCC2 (outward transporter) and NKCC1 (inward transporter), significant alterations of these co-transporters functions were revealed in albino visual cortex neurons, comprising a higher NKCC1 and a lower KCC2 action. Although upregulation of KCC2 and downregulation of NKCC1 are consistent with the significant decrease in intracellular Cl^- observed during postnatal development (Delpire 2000; Ikeda et al. 2003; Staley and Smith, 2001; Yamada et al. 2004; Vardi et al. 2000), additional experiments involving direct measurements of co-transporters actions have to be performed. Interestingly, NKCC1 was reported to be still expressed in the adult human neocortex (immunocytochemistry) (Dzhala et al. 2005) and rat visual cortex (In situ hybridization histochemistry) (Ikeda et al. 2003). Unfortunately it wasn’t found in single adult rat neocortical neurons

(single cell RT PCR and pharmacological blocking) (Yamada et al. 2004). However, if not completely diminished during development, whether or not the co-transporter continues to participate in the regulation of intracellular Cl– in neurons remained to be functionally demonstrated.

Chapter IV

Cation-chloride co-transporters in albino and pigmented rat visual cortex neurons: expressions and functional analysis.

Abstract

In our previous study we demonstrated that albino visual cortex neurons don't show a corresponding decrease in intracellular chloride concentration during the development of their visual cortex as compared to pigmented animals. To uncover the molecular basis for this phenomenon we conducted a single cell real time PCR study of the two most important of the many known chloride regulators in neocortical neurons: the Na^+-K^+-$2Cl^-$ co-transporter (NKCC1, Cl^--uptake) and the K^+-Cl^- co-transporter (KCC2, Cl^--extrusion) in albino and pigmented rat visual cortex neurons coupled with gramicidin perforated patch clamp analysis. 22 out of 31 of albino and 5 out of 30 of pigmented visual cortex neurons were NKCC1 positive. The presence of NKCC1 mRNA strongly correlated with a high intracellular chloride level. Pharmacological blocking of NKCC1 function with 20 micromolar concentration of its selective blocker, bumetanide, caused the population of albino but not pigmented visual cortex cells to display a negative shift in $E_{GABA.}$ In line with this pharmacological effect, NKCC1 mRNA was

found in bumetanide-sensitive neurons, but not in bumetanide-insensitive cells. These data support the idea that NKCC1 may be the main cause of the observed elevated intracellular chloride level in albino visual cortex neurons.

Motivation

Albino mutations are accompanied by specific functional and morphological alterations of the visual system. Resulting abnormalities in albinos affect visual processing including cortical binocularity or direction selectivity in the accessory optic system (Jeffery 1997; Guillery 1986; Akerman et al. 2003; Hoffmann et al. 2002; Hoffmann et al. 2004) Direction selectivity, in turn, critically depends on GABAergic mechanisms (Kittila & Massey 1997; Taylor et al. 2000; Gavrikov et al. 2003; Thiele et al.2004). While GABA is the main inhibitory transmitter in the adult brain, GABAergic transmission is excitatory during early postnatal development. The different actions of GABA result from a reversed chloride concentration gradient with higher intracellular chloride concentration in immature neurons (Ben-Ari, 2002; Payne et al. 2003; Rivera et al. 1999; Yamada et al. 2004). The Na^+-K^+-$2Cl^-$ co-transporter (NKCC1, Cl^--uptake) and the K^+-Cl^- co-transporter (KCC2, Cl^--extrusion) are the most important of the many known chloride

regulators in neocortical neurons (Delpire 2000; Staley & Smith 2001). The developmental switch to an inhibitory action of GABA is believed to be the consequence of a decrease of NKCC1 and increase of KCC2 expression. However, in albino rat visual cortex neurons pharmacologically significant alterations of K^+-Cl^- and Na^+-K^+-Cl^- co-transporters functions were found by using specific blockers: furosemide and bumetanide, comprising a higher NKCC1 and a lower KCC2 action (Barmashenko et al. 2005). This resulted in a shift of the reversal potential of GABAAR-mediated postsynaptic currents into a depolarizing direction in albino rat visual cortical neurons as compared to neurons in visual cortex of pigmented animals.

In the present study we measured the reversal potential of GABAAR-mediated postsynaptic currents and $[Cl^-]_i$ by the gramicidin perforated patch clamp method and examined mRNA expression of NKCC1 (responsible for chloride uptake) and KCC2 (responsible for chloride extrusion) on a single cell level in albino and pigmented rat visual cortex neurons.

Materials and methods

Experiments were carried out on Long-Evans and Wistar rats of postnatal day (P) 21-35. All experimental procedures were strictly in

accordance with institutional guidelines and approved by a local ethics committee. For brain slice preparation and electrophysiological methods refer to chapter III.

Single cell real time PCR

cDNA synthesis and the first round of PCR was performed using the One-Step RT-PCR kit (Qiagen, GmbH, Germany) as described in (Yamada et al. 2004). The kit contains a unique enzyme combination (Omniscript and Sensiscript Reverse Transcriptases) and its specially developed reaction buffer ensures a sensitive (up to 1 pg of RNA), highly specific reverse transcription and PCR in one tube, without the need for optimization. After reverse transcription, reactions are heated to 95°C for 15 minutes to activate HotStarTaq DNA polymerase and simultaneously inactivate the reverse transcriptases. This hot start PCR protocol eliminates any nonspecific amplification products such as primer-dimers and reduces unspecific background products, ensuring a highly sensitive and reproducible RT-PCR. Simultaneous cDNA synthesis and PCR amplification from multiple targets in one tube eliminates the major problem occurring during a two-step single cell RT-PCR (reverse transcription in one tube and PCR in another tube) that

is characterized by the sampling of cDNA from extremely diluted solution.

The cytoplasm of a cell excluding the cell nucleus was aspirated by a single mild suction. This sample was then expelled into a reaction tube, which contained 5µl of RNAse-free water with 10 units of RNAse inhibitor (Qiagen, GmbH, Germany). Harvested cytoplasm was frozen and stored at -80^{o}C for at most 8 hours. The solution for the reverse transcription was prepared by mixing:

10µl of 5x Qiagen OneStep RT-PCR buffer,

2µl of 10mM of each dNTPmix,

1µl of 10µM ß-actin outer primers,

3µl of 10µM KCC2 outer primers,

3µl of 10µl NKCC1 outer primers,

10 units of Qiagen One-Step RT-PCR enzyme mix,

10µl of 5x Q-solution

10µl of RNAse-free water

Afterwards 40 µl of the mixture was combined with the sample and the reverse transcription was performed for 30 min at 50ºC in a thermal cycler. After the reverse transcription step, the first round of PCR

amplification was immediately started in a thermal cycler. It consisted of:

15 min at 95ºC (HotStarTaq DNA Polymerase activation/reverse transcriptases inactivation), followed by 40 cycles of:

30 sec at 94ºC

30 sec at 55ºC

60 sec at 72ºC

Outer primers pair's sequences for NKCC1, KCC2 and ß-actin were taken from (Yamada et al. 2004). The PCR product from ß-actin primers amplified from genomic DNA and pre-mRNA cDNA has a length of 1004 bp while from mature cytoplasmic mRNA it has a length of 543bp (due to the lack of introns, not preserved in mRNA (fig. 4.1A)). It is therefore possible to monitor whether the samples collected from the cells contain unwanted genomic DNA. On agarose gel electrophoresis performed after RT-PCR there was only a single 500 bp product that corresponds to ß-actin primers product from mRNA. There was no band in the region of 1000 bp (see picture 4.1B) indicating the lack of genomic DNA contamination in the samples.

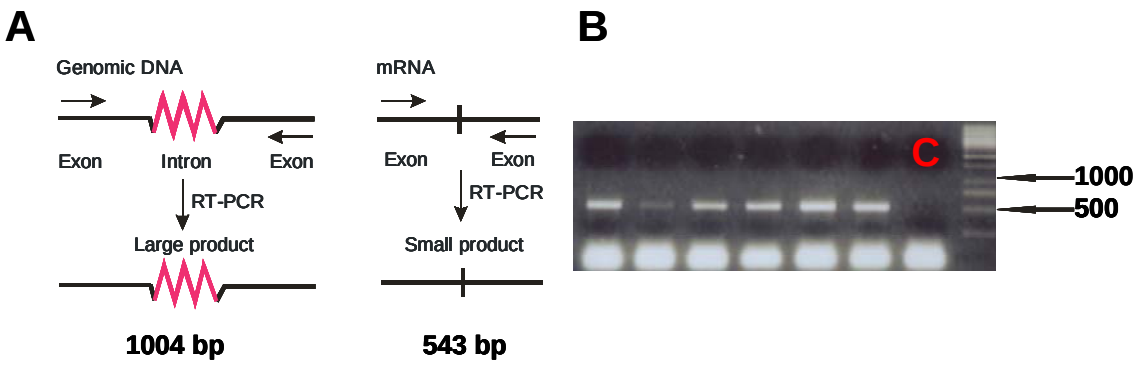

Fig 4.1 A. Schematic representation of primers binding regions in ß-actin genomic DNA and cDNA obtained after reverse transcription of ß-actin mRNA. Note that due to the intron preserved in gDNA but missing in mRNA, the sizes of the final products differ (543 bp and 1004 bp respectively). **B.** Agarose gel electrophoresis of reaction products obtained after the reverse transcription and the first round of PCR (outer primers). Note that there is no visible band in the region of 1004 bp, indicating absence of PCR product from ß-actin genomic DNA. 500bp amplification product corresponds to the PCR product from cDNA of ß-actin (543 bp). Amplification products of KCC2 and NKCC1 are not visible on the gel, because their mRNAs are much lower amplified than ß-actin mRNA.

Subsequently we diluted first-round PCR products 500-fold and 1 µl of the diluted mixture was taken as a template for the second round of PCR (40 cycles) in a real time PCR format using the Opticon2 detection system (Biorad, Hercules, USA) (see fig.4.2 for schematic of experimental procedures). For each template 10µl SyberGreen, 0.25 µl of 10µM inner primers and 9.75 µl of water were used (final reaction volume was 20µl). The amplification involved hot start activation of the

polymerase at 95^{o}C for 10 min, denaturation at 95^{o}C for 15 sec, annealing at 52^{o}C for 30 sec and extension at 72^{o}C for 30 sec in separate reactions using the inner primers pairs (ß-actin, NKCC1, KCC2) for each template. These primers are specific to regions within the PCR products produced by the first round PCR amplification. The design of the inner primers was performed using Primer Express 2.0 software (Applied Biosystems, Foster city, USA). Possible cross-homology between NKCC1, KCC2 and ß-actin sequences was excluded (we used specific primers, see above).

The specificity of primers was further confirmed in agarose gel after amplification and by melting point analysis of the amplicons generated by Real Time PCR. Outer and inner primers sequences are presented in table 4.1.

primers	type	sequence	product length, bp
ß-actin	Outer	5'-ACACGGCATTGTAACCAACT-3' 5'-CATTGCCGATAGTGATGACC-3'	543bp
	Inner	5'-CTAAGGCCAACCGTGAAAAGA-3' 5'-CAACACAGCCTGGATGGCT-3'	86 bp
KCC2	Outer	5'-GATGAAGAAAGACCTGACCA-3' 5'-CTGGTTCAAGTTTTCCCACT-3'	523 bp
	Inner	5'-CAGCGGCTCAGAACAAAG-3' 5'-TTCAAGTTTTCCCACTCCGG-3'	91 bp
NKCC1	Outer	5'-GAAAGTACTCCAACCAGAGA-3' 5'-AGCTAGAATACCAGTTGCAG-3'	720 bp
	Inner	5'-GTGAGAGGAGGAGGAGCATAC-3' 5'-GCGAATCCAACAACATACATAG-3'	125 bp

Table 4.1: Summary of outer and inner primers sequences used in the PCR study

Drugs

The drugs applied were gramicidin D, bumetanide (Sigma, St. Louis, MO), kynurenic acid (KYN, an ionotropic glutamatergic receptor antagonist) and bicuculline (an ionotropic $GABA_A$ receptor antagonist) (Tocris Cookson, Bristol, UK). Substances were prepared as stock solutions and frozen, then added to the ACSF to reach the desired final concentration.

Statistics

Mann-Whitney rank sum test and Chi-square tests ($p < 0.001$), SigmaStat software, were used to test the data for significant disparities. Numerical data are presented as mean ± S.D.

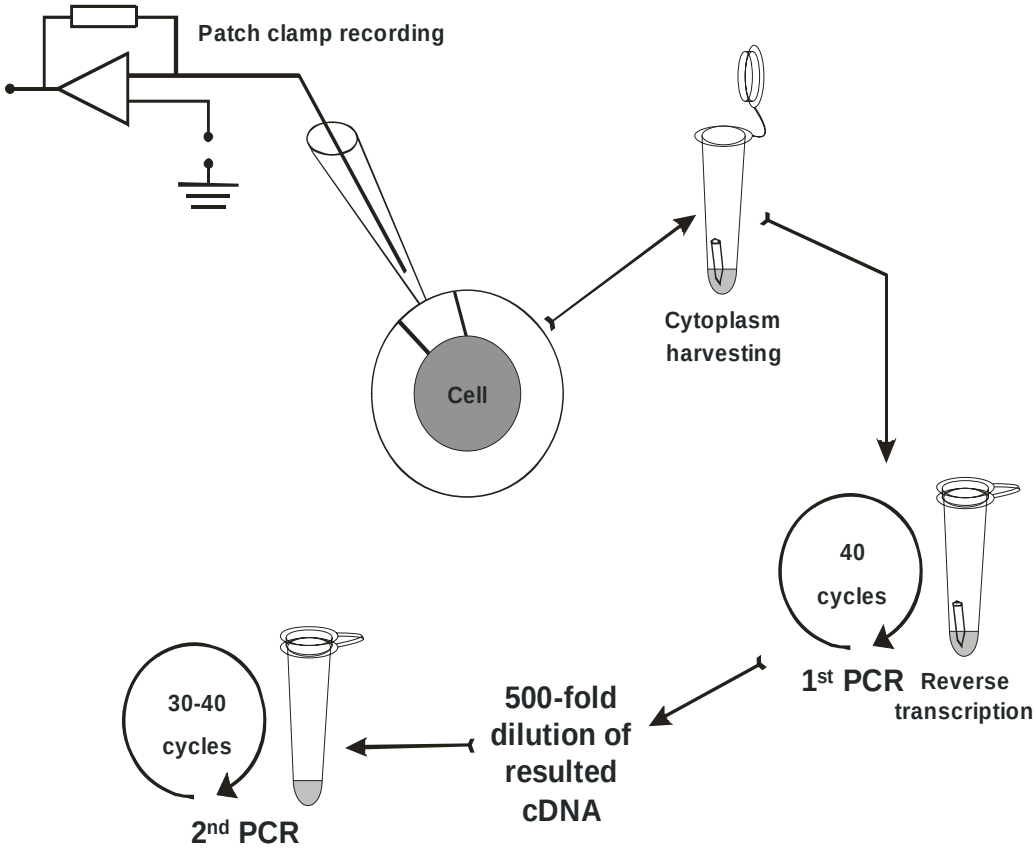

Fig 4.2: Schematic representation of NKCC1, KCC2 and ß-actin expression analysis from single cells. After electrophysiological measurements, cytoplasm of a cell excluding the cell nucleus was aspirated by a single mild suction and expelled into a

reaction tube, which contained RNAse-free water and RNAse inhibitor. Afterwards, the master mix containing components for reverse transcription and PCR, as well as outer primers pairs was combining with the sample. After reverse transcription and 40 cycles of the first round of PCR the mixtures were dissolved 500 times and subjected to the second round of real time PCR with inner primers.

Results

NKCC1 and KCC2 expression analysis in albino and pigmented rat visual cortex neurons

To test whether altered $GABA_AR$ mediated currents observed in albino visual cortex neurons is regulated by the two major cation-chloride co-transporters: KCC2 (outward transporter) and NKCC1 (inward transporter), the mRNAs for these transporters were studied in neurons of the albino and pigmented visual cortex of P20-P40 rats by single cell real time PCR. Out of 61 neurons tested in both control groups (31 for albino and 30 for pigmented), NKCC1 mRNA was found in 27 cells. Of those, 22 neurons were from albino and 5 from pigmented rat visual cortex. ($p<0,001$, Chi-square test, data summarized in table 4.2).

NKCC1 mRNA	+	-	n
Albino neurons	22*	9	31
Pigmented neurons	5	25	30

Table 4.2: Distribution of NKCC1 positive and negative cells as revealed by single cell real time PCR in albino and pigmented rat visual cortex (*p<0,001, Chi-square test).

KCC2 mRNA was detected in every cell tested in both control groups (pigmented and albinos). ß-actin mRNA expression was also found in every cell and served as internal control for PCR efficiency. Sample fluorescence curves of tested PCR products (ß-actin, KCC2 and NKCC1) are presented in fig 4.3, 4.4 and 4.5, correspondingly. Additionally, in the upper left corner of each figure the melting curve analyses of the resultant products is presented.

To investigate whether the observed differences in the co-transporter's expression were also present in non-visual areas we repeated the single cell real time PCR experiments in frontal cortex. We found no NKCC1 mRNA expression at the single cell level in both pigmented (n=3) and albino (n=3) frontal cortex layer 5 cells.

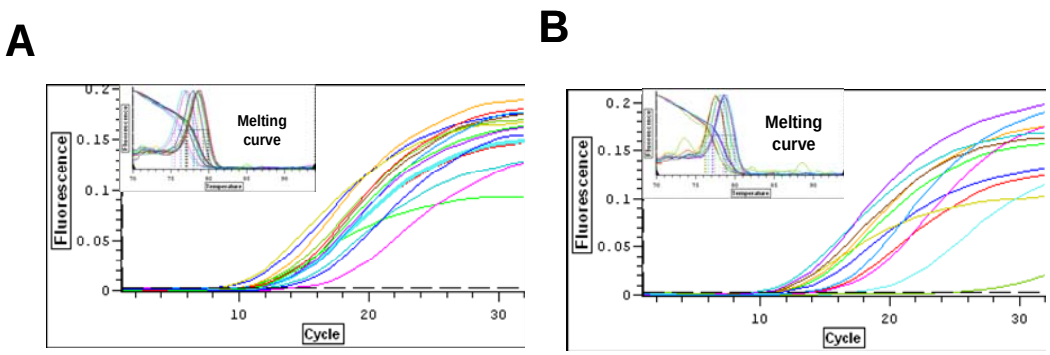

Fig 4.3: Fluorescence curves of PCR products for ß-actin in albino (a) and pigmented (b) visual cortex neurons. After RealTime PCR amplification, products were subjected to melting point analysis (upper left figure on each picture). The temperature was raised stepwise in 1^{o}C increments and hold for 10 sec each. During this time period the change in fluorescence was measured. At the melting point, the two strands of DNA will separate and the fluorescence rapidly decreases. The software plots the rate of change of the relative fluorescence units (RFU) with time (T) (-d(RFU)/dT) on the Y-axis versus the temperature on the X-axis, and this will peak at the melting temperature (Tm). The number of peaks on the melting curve corresponds to the number of products in the tube. Thus a primer-dimer artifact or another non-specific product would give additional peaks. Therefore the single pick in melting curve tells you that there is only one product were synthesized during reaction.

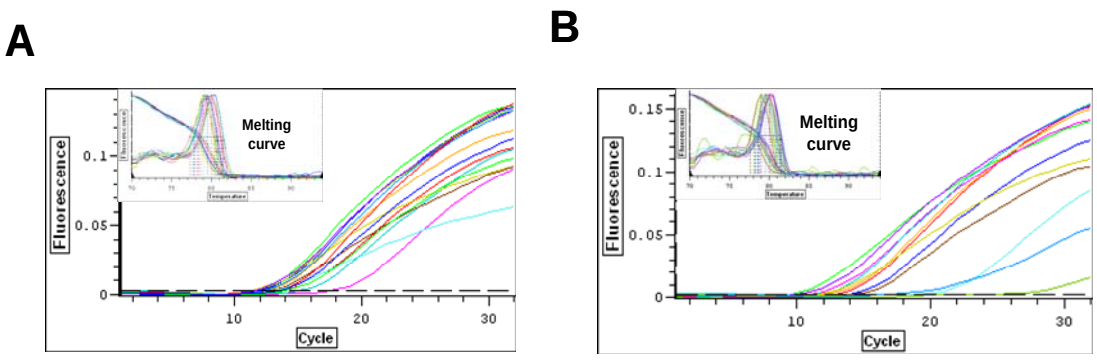

Fig 4.4: Fluorescence curves of PCR products for KCC2 in albino (a) and pigmented (b) visual cortex neurons. The analysis was performed as described above. Note the single peak at the expected melting temperature (Tm) of ~80 ^{o}C corresponding to the KCC2 amplicon.

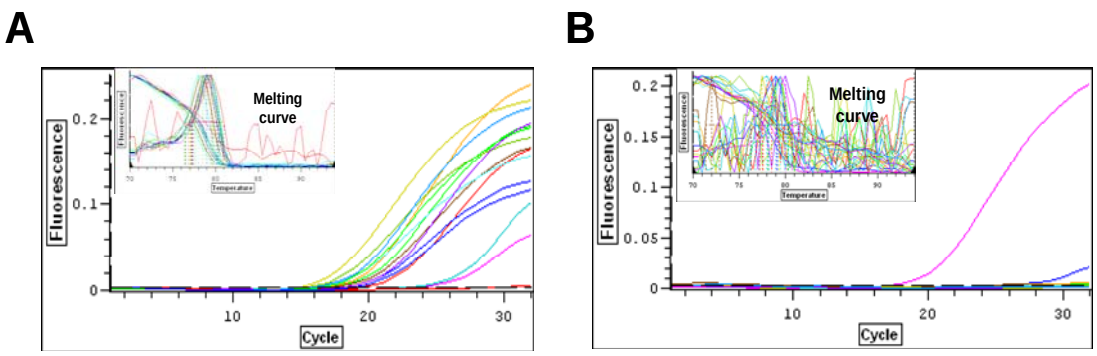

Fig 4.5: Fluorescence curves of PCR products for NKCC1 in albino (a) and pigmented (b) visual cortex neurons. Note that the specific NKCC1 amplicon with the expected Tm of ~79 ^{o}C was almost exclusively found in albino neurons. A single case of a NKCC1 positive neuron is shown in B (purple line).

Correlation of NKCC1 transporter RNA expression in visual cortex to electrophysiology

In order to directly correlate transporter RNA expression to electrophysiology, the following experiments consisted of gramicidin-perforated patch clamp recordings and subsequent analysis of NKCC1 mRNA expression in the cytoplasm of the cells measured. Current–voltage curves of the electrically evoked GABAAR-mediated postsynaptic currents in NKCC1 positive (a) and NKCC1 negative neurons (b) as well as the corresponding sample fluorescence curves of PCR products are presented in fig 4.6. We confirmed a statistically significant difference in the reversal potential of GABAAR-mediated postsynaptic currents between the albino and pigmented rat visual cortical neurons (fig 4.7a): -57+/-6,64mV (n=11) and – 72,6+/-6,93mV (n=10, $p<0,001$, Mann-Whitney rank sum test) respectively. The E_{GABA} value obtained for NKCC1 expressing cells was -56,1+/-6,00 (n=10), while for NKCC1 negative neurons this value comprised -72+/-7,07 (n=11, $p<0,001$, Mann-Whitney rank sum test) (fig 4.7b). Additionally, the presence of NKCC1 RNA strongly correlated with high intracellular chloride level as summarized in figure 4.8. By application of the $GABA_AR$ antagonist bicuculline (30 μM) all PSCs disappeared.

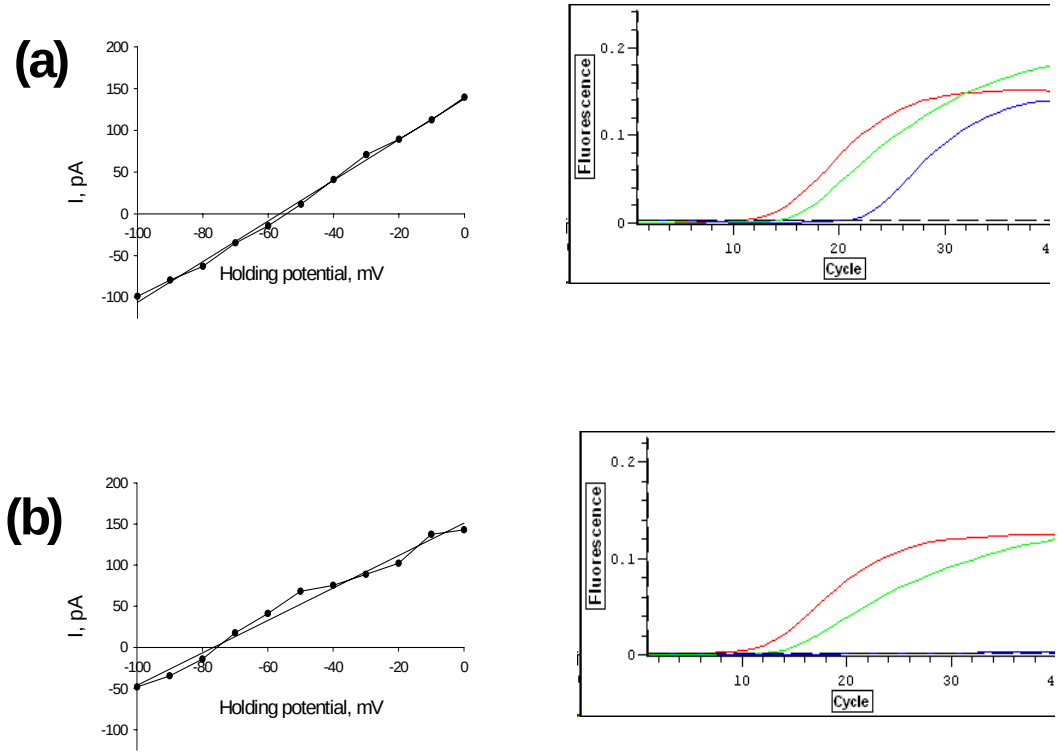

Fig 4.6: Sample current–voltage curves of the electrically evoked GABAAR-mediated postsynaptic currents and fluorescence curves of tested PCR products (red trace for ß-actin, green for KCC2 and blue for NKCC1) in NKCC1 positive **(a)** and NKCC1 negative visual cortex neurons **(b)**. Note the E_{GABA} shift in positive direction in NKCC1 positive neurons.

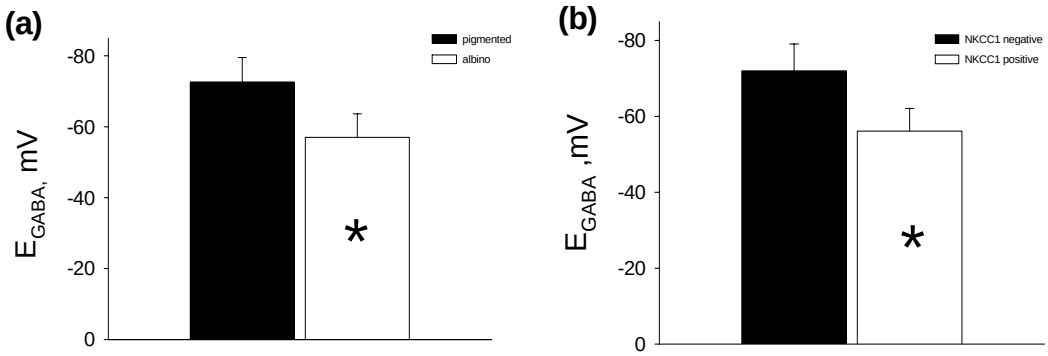

Fig 4.7: Differences in the reversal potential of GABAAR-mediated postsynaptic currents between albino and pigmented rat visual cortex neurons **(a)** and NKCC1 positive and negative cells **(b)**. Data are presented as mean ±S.D (*p<0,001, Mann-Whitney rank sum test).

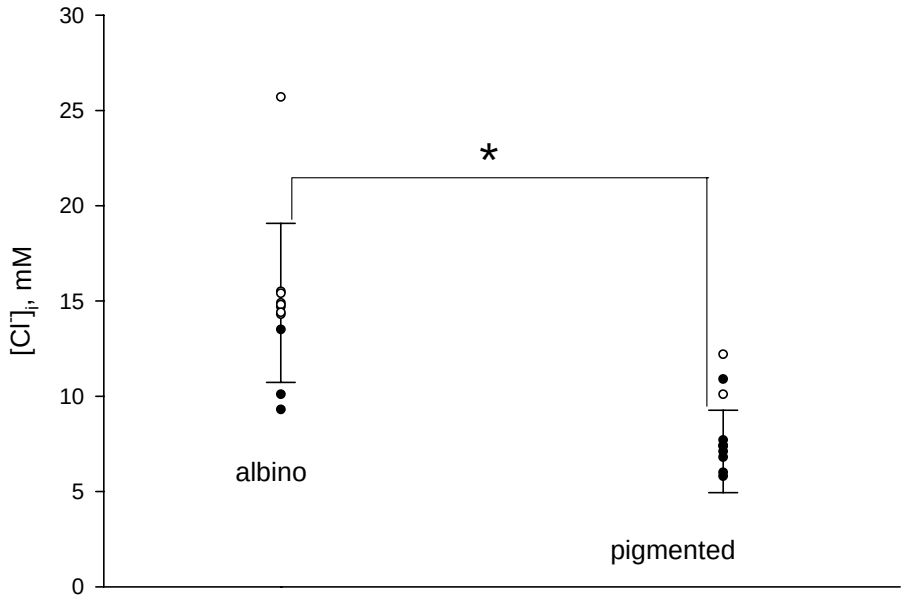

Fig 4.8: Relationship between $[Cl^-]_i$ level and expression of NKCC1 co-transporter in albino and pigmented rat visual cortex neurons. Open circles represent NKCC1 negative cells, full circles – positive. Data are presented as mean ±S.D (*p<0,001, Mann-Whitney rank sum test).

Determination of Na-K-Cl co-transporter activity in albino visual cortical neurons

In the presence of 10 micromolar concentration of bumetanide, a specific inhibitor of the NKCC1 co-transporter, cells with more positive values of E_{GABA} than usual for neocortical neurons displayed a negative shift in E_{GABA}. A negative shift in E_{GABA} was observed in 7 out of 9 of albino visual cortex neurons and 1 out of 7 neurons from pigmented animals (data are summarized in fig 4.9a). In line with this pharmacological effect, NKCC1 mRNA was expressed in bumetanide-sensitive neurons, but not in bumetanide-insensitive ones. Calculated contribution of NKCC1 action to the reversal potential of GABAAR-mediated postsynaptic currents for albino and pigmented rat visual cortex neurons presented in figure 4.9b.

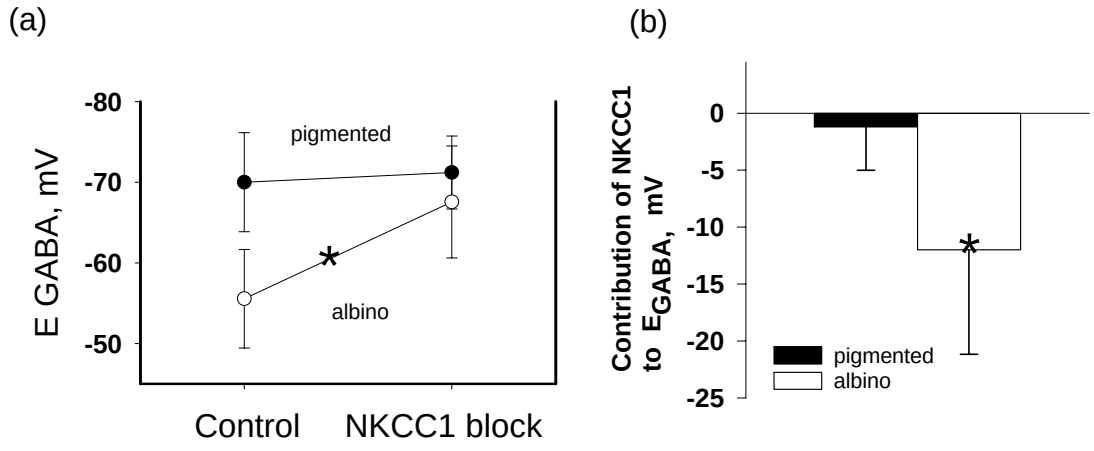

Fig 4.9: Effects of NKCC1 blocking (a) and calculated contribution of NKCC1 action (b) to the reversal potential of GABAAR-mediated postsynaptic currents for albino and pigmented rat visual cortex neurons. Data are presented as mean ± S.D ($^{*}p<0,001$, Mann-Whitney rank sum test).

Discussion

The change in the GABA response from a depolarizing to a hyperpolarizing direction during development depends on intracellular Cl^- concentration.

An inhibitory action of GABA is required to discriminate differences in input activities during processes accompanied by synaptic pruning, such as segregation and the formation of ocular-dominance columns (Ikeda et al. 2003). Furthermore, the presence of GABAA receptor-mediated inhibition is essential during the critical period of ocular-dominance

plasticity (Hensch et al. 1998). In addition, only if the level of GABAergic inhibition is within a certain range ("window") the critical period can occur (Fagiolini & Hensch 2000). When the release of GABA is reduced, as in GAD65-knockout mice (Hensch et al. 1998), the critical period does not occur at all, whereas diazepam induced enhancement of GABA-receptor-mediated activity allows generation of the critical period at any time (Fagiolini & Hensch 2000). This process of activity-dependent development is so sensitive to GABA-receptor-mediated inhibitory tonus that it might be modulated by changes in Cl- homeostasis.

Interestingly in cortical neurons, a shift in Cl- homeostasis toward a higher $[Cl-]_i$ is implicated in the determination of specific developmental stages because the resulting depolarizing GABAergic and glycinergic responses mediate various developmental processes, such as neuronal migration, differentiation, and synapse formation (Ben-Ari 2002; Behar et al. 1996,1998; Owens & Kriegstein 2003).

The two most important of the many known chloride regulators in neocortical neurons are: the Na^+-K^+-$2Cl^-$ co-transporter and the K^+-Cl^- co-transporter (Delpare 2000; Staley & Smith 2001). The developmental switch to an inhibitory action of GABA is a consequence of a decrease of NKCC1 and increase of KCC2 expression. Cl^- uptake in immature

neurons is mediated by Na^+-K^+-$2Cl^-$ co-transporter (Payne et al. 2003; Yamada et al. 2004; Stein & Nicoll 2003), and moreover no $GABA_A$ mediated depolarization was found in NKCC1 knock out mice (Sung et al. 2000).

Expression of NKCC1 is high at birth and decreases during postnatal development (Rivera et al. 1999; Plotkin et al. 1997) and is responsible for depolarizing and excitatory action of GABA and glycine in immature neurons (Yamada et al. 2004; Kakazu et al. 1999). In contrast to NKCC1, the central role of KCC2 co-transporter is promoting inhibition and preventing hyperexcitability (Rivera et al. 1999; Rivera et al. 2005). Zhu et al. (2005) showed in a $KCC2^{-/-}$ mouse model that cortical neurons lacking KCC2 not only fail to show a developmental decrease in $[Cl^-]_i$, but also are unable to regulate $[Cl^-]_i$ on Cl^- loading or to maintain $[Cl]_i$ during membrane depolarization.

The present study describes and compares intracellular chloride homeostasis in albino and pigmented rat visual cortex neurons by means of electrophysiological, molecular and pharmacological analysis. On the molecular biological level we found that the most important chloride regulator responsible for chloride uptake - Na^+-K^+-$2Cl^-$ co-transporter (Payne et al. 2003; Delpire 2000) is not downregulated in P20-40 albino visual cortex neurons. Our electrophysiological data showed significant

differences in GABAergic mechanisms in albino visual cortex comprising shifted reversal potential of GABAAR-mediated postsynaptic currents into depolarizing direction in albino rat visual cortex neurons as compared to pigmented animals (these data are consistent with resent findings published by Barmashenko et al. in 2005). Our pharmacological tests confirmed that the observed inhibitory deficit in albino visual cortex neurons on the electrophysiological level and the mRNA expression of the major chloride regulator responsible for chloride uptake on single cell molecular biological level isn't just a correlation but causal relationship.

After pharmacological block of the co-transporter, reversal potential of electrically evoked GABAAR-mediated postsynaptic currents and, as inferred from these measurements, $[Cl^-]_i$ in albino visual cortex neurons shifted to values similar to those found in the neurons of visual cortex in pigmented rats. Interestingly, we detected several NKCC1 positive neurons in P20-40 pigmented rat visual cortex as well. This is in contrast to Yamada et al. (2004) (method: semiquantitative single cell multiplex RT PCR). They did not find any NKCC1 mRNA in P11-20 rat neocortical neurons. However, NKCC1 was found in adult human neocortex (Dzhala et al. 2005) and in rat visual cortex (Ikeda et al. 2003)

using other methods. The functional role of NKCC1 in adult neocortex remains to be determined and demands further investigations.

We found KCC2 mRNA in every cell tested in both pigmented and albino visual cortex. It is possible to argue that the expression of the major outward chloride co-transporter is not impaired, or is not impaired to such an extent as its inward counterpart. As our two-steps real-rime single cell PCR didn't reveal qualitative difference in KCC2 mRNA expression and there is no reliable co-transporter blocker available (Rivera et al. 2005), further investigations may be needed to quantify this co-transporter's participation in intracellular chloride regulation in albino visual cortex neurons compared to neurons in the visual cortex of pigmented rats.

Chapter V

Changes in E_{GABA} in visual cortex of pigmented and albino rats after metabotropic glutamate receptors block

Abstract

In a previous study we investigated the expression of the two most important of the many known chloride regulators in neocortical neurons: the Na^+-K^+-$2Cl^-$ co-transporter (NKCC1, Cl^--uptake) and the K^+-Cl^- co-transporter (KCC2, Cl^--extrusion) in albino and pigmented rat visual cortex neurons. We showed that the most important chloride regulator responsible for chloride uptake – the Na^+-K^+-$2Cl^-$ co-transporter was not downregulated and remained functional shifting GABAergic transmission into the depolarizing direction in P20-40 albino visual cortex neurons as compared to pigmented animals. There were reports of enhancement of the Na-K-Cl co-transporter activity in the presence of metabotropic glutamate receptor agonists. Therefore, in this study we investigated the contribution of the metabotropic glutamate receptors (mGluR) to the observed changes. Using perforated patch clamp methods we revealed a significant shift of E_{GABA} towards hyperpolarization by block of metabotropic glutamate receptors in albinos, but not in pigmented animals. After the mGluR block E_{GABA} in

albino visual cortex neurons was not statistically different from that in pigmented animals.

Motivation

Depolarizing action of GABA subsequently activates *N*-methyl-D-aspartate (NMDA) and voltage-gated Ca^{2+} channels that leads to a rise in intracellular Ca^{2+} and activation of a wide range of intracellular cascades (Ben-Ari et al. 1997). In addition, the pure opening of NMDA receptors was found to increase the NKCC1 activity in a Ca^{2+}-dependent manner (Sun & Murali, 1999). Na^{+}-K^{+}-$2Cl^{2-}$ co-transporter in immature cortical neurons is regulated by group-I mGluR- and AMPA receptor–mediated signal transduction pathways and the mGluRs-mediated stimulation of the co-transporter is dependent on a rise of intracellular Ca^{2+} and activation of Ca^{2+}/CaM kinase II. (Sun & Murali, 1999; Schomberg et al. 2001). Thus, Schomberg et al. in 2001, reported that significant stimulation of the co-transporter activity was observed in the presence of both trans-(6)-1-aminocyclopentanetrans-1,3-dicarboxylic acid (trans-ACPD), a metabotropic glutamate receptor agonist, and (RS)-3,5-dihydroxyphenylglycine (DHPG), a selective group-I mGluR agonist.

In addition, DHPG-induced stimulation of the co-transporter activity was inhibited in the presence of mGluRs antagonist (RS)-1-aminoindan-1,5-dicarboxylic acid (AIDA) and also with selective mGluR1 antagonist 7-(hydroxyimino)cyclopropa-[b]chromen-1a-carboxylate ethyl ester (CPCCOEt).

DHPG-mediated stimulation of the co-transporter was abolished by inhibition of Ca^{2+}/CaM kinase II. Moreover, the loss of intracellular Cl^- mediated by the $GABA_A$ receptor stimulates NKCC1 activity (Schomberg et. al., 2003).

In this work, using the perforated patch clamp technique, we revealed a significant shift of E_{GABA} towards hyperpolarization by block of metabotropic glutamate receptors in albinos, but not in pigmented animals.

Materials and methods

Experiments were carried out on Long-Evans and Wistar rats of postnatal day (P) 21-35. All experimental procedures were strictly in accordance with institutional guidelines and approved by a local ethics committee. For brain slice preparation and electrophysiological methods refer to chapter III.

Drugs

The drugs applied were a-methyl-4-carboxyphenylglycine (MCPG, a metabotropic glutamatergic receptor antagonist), kynurenic acid (KYN, an ionotropic glutamatergic receptor antagonist), bicuculline (an ionotropic $GABA_A$ receptor antagonist) and picrotoxin citrate (an ionotropic GABA receptor antagonist) (Tocris Cookson, Bristol, UK). Substances were prepared as stock solutions and frozen, then added to the ACSF to reach the desired final concentration. Kynurenic acid was added directly to the bath solution to prevent excitatory activity in the neurons tested.

Data acquisition and calculating

For recording and analyzing WinWCP software (John Dempster, University of Strathclyde, Glasgow, UK) was used. One way ANOVA ($p < 0.001$), SigmaStat 2.03 software, was used to test the data for significant disparities. Numerical data are presented as mean ± S.D.

Results

All recorded cells were pyramidal shaped neurons from layer V of visual cortex. In our experiments we investigated $GABA_A$ receptor mediated currents before and after metabotropic glutamate receptors block with a-methyl-4-carboxyphenylglycine (MCPG, 500 μM). mGluR block significantly shifted reversal potential of the $GABA_A$ receptor mediated currents (E_{GABA}) to hyperpolarizing direction in albino ($p<0,001$), but did not change it in pigmented animals (Fig. 5.1A). Calculated values of intracellular chloride were 9,93+/-0,83 mM in pigmented and 16,01+/-0,97 mM in albino rats ($p<0,001$) before and 9,84+/-1,11 mM and 10,42+/-1,19 mM after mGluR block ($p>0,5$) (fig 5.1B). Intracellular chloride levels for the above mentioned groups were calculated from the $GABA_AR$ mediated currents reversal potential according to the Nernst equation ($T=25^oC$). Shift of E_{GABA} after mGluR block with MCPG (500 μM) was significantly greater ($p<0,001$) in rats with high intracellular chloride concentration (albino, n=10) than in control (pigmented, n=8) animals. E_{GABA} in albino rats was considerably more depolarized in comparison to pigmented animals (-54,63±2,04 vs. -69,00±2,32 mV, $p<0,001$).

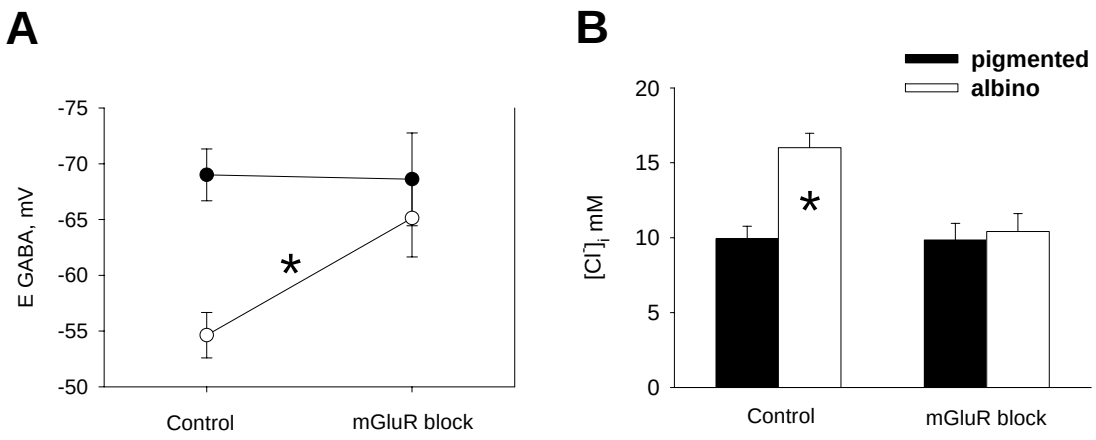

Fig 5.1: (A) Changes in E_{GABA} in visual cortex after mGluR block in pigmented (full symbols) and albino (open symbols) rats. Note that E_{GABA} was significantly hyperpolarized by the mGluR current block in albinos, but was not changed in pigmented animals. **(B)** Estimation of intracellular chloride concentration ($[Cl^-]_i$) in visual cortex neurons of albino and pigmented rats, before and after mGluR block with 500 μM of MCPG, T=25^{o}C. Data are presented as mean ±S.D ($^*p<0,001$, one way ANOVA).

In this work we investigated the impact of metabotropic glutamate receptors (all ionotropic excitatory currents we blocked with kynurenic acid) onto intracellular chloride concentration in neurons of the visual cortex of albino rats. Albino Wistar rats have changed $GABA_AR$ mediated currents in visual cortex neurons compared to pigmented Long Evans animals (Barmashenko et. al., 2005). Here we showed significant shift of E_{GABA} to hyperpolarizing induced by block of mGluR in albinos, but not in control animals (pigmented), see fig 5.1A. Contribution of

mGluR to E_{GABA} in neurons of pigmented (Norma) and albino (high NKCC1 action) rats is presented on Fig 5.2.

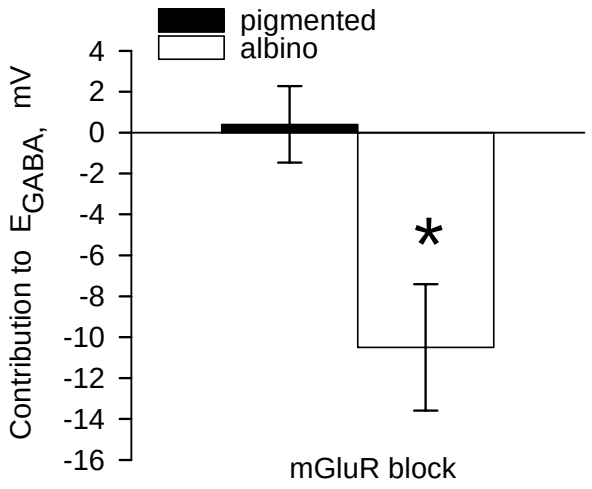

Fig 5.2 mGluR contribution to E_{GABA} in visual cortex neurons of pigmented (full bars) and albino (open bars) rats. Data are presented as mean ±S.D ($^{*}p<0,001$, one way ANOVA).

Discussion

The change of GABAergic and glycinergic mediated responses from depolarizing to hyperpolarizing is a consequence of change in the driving force for Cl^- and a shift in GABA and glycine reversal potential during development (Ben-Ari, 2002; Payne et al. 2003; Rivera et al. 1999). Interestingly, $GABA_A$-mediated depolarizing currents may reappear at the dendrites but not at cell bodies of mature neurons, this

current is mediated by the outward movement of HCO^-_3 ions through the $GABA_A$ receptor/Cl^- channel (Staley & Proctor, 1999). Permeability of the $GABA_A$ receptor to HCO^-_3 is ~1/5 of the permeability to Cl^- (Delpire, 2000). Contribution of HCO^-_3 to GABA currents is difficult to estimate in the presence of a strong driving force for Cl^- in physiological condition, but definitely it is lower than 1/5. Not excluding the importance of other Cl^- transport pathways (the Cl^-/HCO^-_3 – exchanger and some Cl^- channels such as ClC2, which has not been found in cortical neurons), one can assume that the action of the cation-chloride co-transporters is the main source for the maintenance of Cl^- homeostasis in neurons. The Na^+-K^+-$2Cl^{2-}$ co-transporter in cortical neurons is regulated by group-I mGluR- and AMPA receptor–mediated signal transduction pathways (Sun & Murali, 1999; Schomberg et. al., 2001). Upregulation of KCC2 and downregulation of NKCC1 are consistent with the significant decrease in intracellular Cl^- observed during postnatal development (Delpire, 2000; Staley and Smith, 2001; Ikeda et al. 2003; Yamada et al. 2004; Vardi et al. 2000).

Here we showed that mGluR block in albinos changed their depolarized E_{GABA} to a normal physiological state (fig. 5.1A). This might be caused by dependent action of NKCC1 and group-I mGluR. Na^+-K^+-$2Cl^{2-}$ co-transporter in cortical neurons is regulated by group-I mGluR- and

AMPA receptor–mediated signal transduction pathways (Sun & Murali, 1999; Schomberg et al., 2001).

As far as shifted E_{GABA} induced by blocking of mGluR in albino neurons and, as a consequence intracellular chloride level, were not statistically distinguishable from those of pigmented without mGluR block (see fig. 5.1A&B) one can propose also from this experiment that the main dysfunctions of albino visual cortex neurons are due to a higher NKCC1 action.

Chapter VI

General Conclusions

First study (Chapter III):

In our first study we monitored the reversal potential of $GABA_A$ receptor mediated currents during postnatal development in both albino and pigmented visual cortex neurons and showed that after the second week of postnatal development neurons in the visual cortex of albinos start to remain at a more positive reversal potential of $GABA_A$ receptor mediated currents when compared to pigmented animals. Furthermore, we proved that strain variations don't contribute to the observed differences. This finding supports the hypothesis of an aberrant maturation of albino visual circuits rather than the existence of inborn abnormalities. Functional analysis of this phenomenon reveals hyperexcitability in albino visual cortex neurons and indicates that albino visual cortex networks may show reduced opportunity for high frequency neuronal coding.

Second study (Chapter IV):

In our second study, using a combined electrophysiological, pharmacological and molecular biological approach, we revealed a qualitative difference in NKCC1, but not KCC2 mRNA expression between albino and pigmented rat visual cortex neurons. We determined

a positive relationship between the presence of NKCC1 and reversal potential of electrically evoked GABAAR-mediated postsynaptic currents shifted to depolarization direction in albino visual cortex neurons. Furthermore our pharmacological experiments involving blockade of NKCC1 function with its specific inhibitor, bumetanide, during electrophysiological recordings and subsequent single cell real time PCR analysis of the co-transporter mRNA linked the inhibitory deficit observed in albino visual cortical network almost exclusively to the high expression of NKCC1. After pharmacological block of the co-transporter, reversal potential of electrically evoked GABAAR-mediated postsynaptic currents and, as a correlate, $[Cl-]_i$ in albino visual cortex neurons shifted to values as found in a pigmented rat's visual cortex. These data support the idea that NKCC1 may be the leading cause for the observed elevated intracellular chloride level in albino visual cortex neurons.

Third study (Chapter V):

It is known that metabotropic glutamate receptor (mGluR) agonists enhance the Na-K-Cl co-transporter activity. In our third study we revealed that mGluR antagonist causes a significant shift of E_{GABA} to hyperpolarizing direction in albinos (expressing NKCC1 mRNA), but not in pigmented visual cortex neurons (not expressing NKCC1

mRNA). After block of mGluR in albino visual cortex neurons, E_{GABA} and the corresponding intracellular chloride level were not statistically distinguishable from those of neurons in visual cortex of pigmented rats before mGluR blockade. These findings strengthen our hypothesis that the changed Cl homeostasis is due to the action of NKCC1

Based on these results I propose a model of regulation of the most important chloride transporter responsible for chloride uptake - Na^+-K^+-$2Cl^-$ co-transporter in albino visual cortex neurons (fig 6.1C). In fig 6.1A and 6.1B the known mechanisms of NKCC1 and KCC2 actions and their contributions in $[Cl^-]_i$ in immature and mature neurons are presented. As our molecular biological approach didn't reveal a qualitative difference in KCC2 mRNA expression and there is no reliable blocker of K-2Cl- co-transporter function available, further investigations may be needed to quantify this co-transporter's participation in intracellular chloride regulation in albino visual cortex neurons compared to visual cortex neurons in pigmented animals. However, because (1) we found KCC2 mRNA in every cell tested in both pigmented and albino visual cortex, (2) pharmacological experiments showed that blockade of the Na-K-Cl co-transporter shifted $[Cl^-]_i$ in albino visual cortex neurons to a value comparable neurons in the visual cortex of pigmented rats, one may argue that the regulation of

the major outward chloride co-transporter is not impaired, or impaired not to such an extent as its inward counterpart.

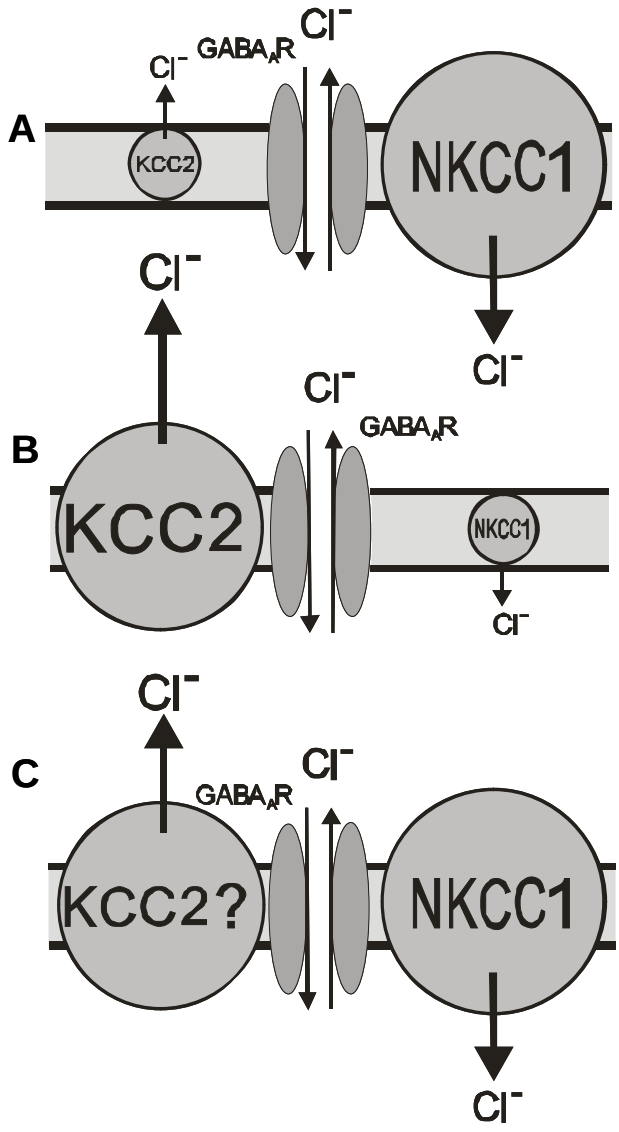

Fig 6.1: Mechanism of NKCC1 and KCC2 actions and their contributions in [Cl-]i in (A) immature neuron, high NKCC, low KCC activity; (B) mature neuron, low NKCC1, high KCC2 activity; (C) proposed model of Cl regulation in albino visual cortex: high NKCC1 action, whether KCC2 action differs from healthy brain remains to be determined.

References

Akerman, C.J., Tolhurst, D.J., Morgan, J.E., Baker, G.E., and Thompson, I.D. (2003). Relay of Visual Information to the Lateral Geniculate Nucleus and the Visual Cortex in Albino Ferrets. *J Comp Neurol.* **461(2),** 217-35.

Apkarian, P. (1992) A practical approach to albino diagnosis. VEP misrouting across the age span. *Ophthalmic Paediatr Genet.***13,** 77–88.

Apkarian, P., Reits, D., Spekreijse, H., Van Dorp, D. (1983) A decisive electrophysiological test for human albinism. *Electroencephalogr Clin Neurophysiol* **55,** 513-531.

Barmashenko, G., Schmidt, M., Hoffmann, K.P. (2005) Differences between cation-chloride co-transporter functions in the visual cortex of pigmented and albino rats. *Eur. J. Neurosci.,* **21,** 1189–1195.

Behar, T.N., Li, Y.X., Tran, H.T., Ma, W., Dunlap, V., Scott, C., Barker, J.L. (1996) GABA stimulates chemotaxis and chemokinesis of embryonic cortical neurons via calcium-dependent mechanisms. *J. Neurosci*, **16,** 1808–1818.

Behar, T.N., Schaffner, A.E., Scott, C.A., O'Connell, C., Barker, J.L. (1998) Differential response of cortical plate and ventricular zone cells to GABA as a migration stimulus. *J. Neurosci*, **18,** 6378–6387.

Ben-Ari, Y. (2002) Excitatory actions of gaba during development: the nature of the nurture. *Nat. Rev. Neurosci.,* **3(9),** 728-39. Review.

Ben-Ari, Y., Khazipov, R., Leinekugel X., Caillard, O., Gaiarsa, J. (1997) GABAA, NMDA and AMPA receptors: a developmentally regulated 'menage a trois.' *Trends Neurosci* **20,** 523–529.

Buzsáki, G. (2001) Hippocampal GABAergic interneurons: a physiological perspective. *Neurochem Res,* **26(8-9),** 899-905.

Cooper, M.L., Blasdel, G.G. (1980). Regional variation in the representation of the visual field in the visual cortex of the Siamese cat. *J Comp Neurol.* **193(1),** 237-53.

Creel, D.J. (1971) Visual system anomaly associated with albinism in the cat. *Nature* **231,** 465-466.

Creel, D.J., Summers, C.G., King, R.A. (1990) Visual anomalies associated with albinism. *Ophthalmic Paediatr Genet.* **11(3),** 193-200.

Creel, D.J., Witkop, C.J., King, R.A. (1974) Asymmetric visually evoked potentials in human albinos: evidence for visual system anomalies. *Invest Ophthalmol Vis Sci,* **13(6),** 430-440.

Delpire, E. (2000) Cation-Chloride Cotransporters in Neuronal Communication. *News Physiol Sci.* **15**, 309-312.

Dzhala, V.I., Talos, D.M., Sdrulla, D.A., Brumback, A.C., Mathews, G.C., Benke, T.A., Delpire, E., Jensen, F.E., Staley, K.J. (2005) NKCC1

transporter facilitates seizures in the developing brain. *Nat Med.*, **11(11),** 1205-13.

Ehrlich, I., Lohrke, S., Friauf, E. (1999) Shift from depolarizing to hyperpolarizing glycine action in rat auditory neurones is due to age-dependent Cl– regulation. *J Physiol (Lond)* **520,** 121–137.

Fagiolini, M., Hensch, T.K. (2000) Inhibitory threshold for critical-period activation in primary visual cortex. *Nature*, **404(6774),** 183-6.

Gamba, G., Miyanoshita, A., Lombardi, M., Lytton, J., Lee, W.S., Hediger, M.A., Hebert, S.C. (1994) Molecular cloning, primary structure, and characterization of two members of the mammalian electroneutral sodium-(potassium)-chloride cotransporter family expressed in kidney. *J Biol Chem*, **269(26),** 17713-22.

Ganguly, K., Schinder, A.F., Wong, S.T., Poo, M. (2001) GABA itself promotes the developmental switch of neuronal GABAergic responses from excitation to inhibition. *Cell*, **105(4),** 521-32.

Gavrikov, K.E., Dmitriev, A.V., Keyser, K.T., Mangel, S.C. (2003) Cation-chloride cotransporters mediate neural computation in the retina. *Proc. Natl. Acad. Sci. USA*, **100,** 16047-16052.

Grichtchenko, I.I., Choi, I., Zhong, X., Bray-Ward, P., Russell, J.M., Boron, W.F. (2001) Cloning, characterization, and chromosomal mapping of a human electroneutral Na(+)-driven Cl-HCO3 exchanger. *J Biol Chem*, **276(11),** 8358-63.

Guillery, R.W. (1986) Neural abnormalities of albinos. *Trends Neurosci.* **18,** 364-367.

Guillery, R.W., Hickey, T.L., Kaas, J.H., Felleman, D.J., Debruyn, E.J., Sparks, D.L. (1984). Abnormal central visual pathways in the brain of an albino green monkey (*Cercopithecus aethiops*). *J Comp Neurol* **226,** 165–183.

Guillery, R.W., Kaas, J.H. (1973) Genetic abnormality of the visual pathways in a "white" tiger. *Science* **180,** 1287-1289.

Guillery, R.W., Okoro, A.N., Witkop, C.J. Jr (1975) Abnormal visual pathways in the brain of a human albino. *Brain Res***, 96,** 373-377.

Hedera, P, Lai, S, Haacke, E.M., Lerner, A.J., Hopkins, A.L., Lewin, J.S., Friedland, R.P. (1994) Abnormal connectivity of the visual pathways in human albinos demonstrated by susceptibility-sensitized MRI. *Neurology,* **44(10),** 1921-6.

Hensch, T.K., Fagiolini, M., Mataga, N., Stryker, M.P., Baekkeskov, S., Kash, S.F. (1998) Local GABA circuit control of experience-dependent plasticity in developing visual cortex. *Science*, **282(5393),** 1504-8.

Hoffmann, K.P., Bremmer, F., Thiele, A., Distler, C. (2002). Directional asymmetry of neurons in cortical areas MT and MST projecting to the NOT-DTN in macaques. *J Neurophysiol.* **87(4),** 2113-23.

Hoffmann, K.P., Garipis, N., Distler, C. (2004) Optokinetic deficits in albino ferrets (Mustela putorius furo): a behavioral and electrophysiological study. *J. Neurosci.,* **24,** 4061-4069.

Hoffmann, K.-P., Stone, J. (1985) Retinal input to the nucleus of the optic tract of the cat assessed by antidromic activation of ganglion cells. *Exp. Brain. Res*., **59**, 395-403.

Hoffmann, M.B., Tolhurst, D.J., Moore, A.T., Morland, A.B. (2003). Organization of the Visual Cortex in Human Albinism. *J Neurosci.* **23(26),** 8921– 8930.

Hubel, D.H., Wiesel, T.N. (1971) Aberrant visual projections in the Siamese cat. *J Physiol.* **218(1),** 33-62.

Ikeda, M., Toyoda, H., Yamada, J., Okabe, A., Sato, K., Hotta, Y., Fukuda, A. (2003) Differential development of cation-chloride cotransporters and Cl- homeostasis contributes to differential GABAergic actions between developing rat visual cortex and dorsal lateral geniculate nucleus. *Brain Res.* **984(1-2),** 149-59.

Ilia, M., Jeffery, G. (2000) Retinal cell addition and rod production depend on early stages of ocular melanin synthesis. *J Comp Neurol.,* **420(4),** 437-44.

Jeffery, G. (1997). The albino retina: an abnormality that provides insight into normal retinal development. *Trends Neurosci.* **20(4),** 165-9.

Jeffery, G., Schütz, G., Montoliu, L. (1994) Correction of abnormal retinal pathways found with albinism by introduction of a functional tyrosinase gene in transgenic mice. *Dev Biol,* **166(2),** 460-4.

Kaas, J.H., Guillery, R.W. (1973). The transfer of abnormal visual field representations from the dorsal lateral geniculate nucleus to the visual cortex in Siamese cats. *Brain Res.* **59,** 61-95.

Kaila, K. (1994) Ionic basis of GABAA receptor channel function in the nervous system. *Prog. Neurobiol,* **42,** 489–537.

Kakazu, Y., Akaike, N., Komiyama, S., Nabekura, J. (1999) Regulation of intracellular chloride by cotransporters in developing lateral superior olive neurons. *J Neurosci,* **19(8),** 2843-51.

Karadsheh, M.F., Delpire, E. (2001) Neuronal restrictive silencing element is found in the KCC2 gene: molecular basis for KCC2-specific expression in neurons. *J Neurophysiol,* **85(2),** 995-7.

Kasmann-Kellner, B., Schafer, T, Krick, C.M., Ruprecht K.W., Reith, W, Schmitz, B.L. (2003). Anatomical differences in optic nerve, chiasma and tractus opticus in human albinism as demonstrated by standardised clinical and MRI evaluation. *Klin Monatsbl Augenheilkd.* **220(5),** 334-44.

Kinnear, P. E., Jay, B., Witkop, C. J. (1985) Albinism. *Surv. Ophthalmol.* **30**, 75–101.

Kittila, C.A., Massey, S.C. (1997) Pharmacology of directionally selective ganglion cells in the rabbit retina. *J. Neurophysiol*, **77,** 675-689.

Kriss, A, Russell-Eggitt, I, Harris, C.M., Lloyd, I.C., Taylor, D. (1992). Aspects of albinism. *Ophthalmic Paediatr Genet.***13(2),** 89-100.

Lannou J., Cazin L., Precht W., Toupet M. (1982) Optokinetic, vestibular, and optokinetic-vestibular responses in albino and pigmented rats. *Pflugers Arch.*, **393,** 42-44.

Leventhal, A.G., Creel, D.J. (1985). Retinal projections and functional architecture of cortical areas 17 and 18 in the tyrosinase-negative albino cat. *J Neurosci.* **5(3),** 795-807.

Lund, R.D. (1965) Uncrossed visual pathways of hooded and albino rats. *Science* **149,** 1506-1507.

Mazzoni, A., Broccard, F.D., Garcia-Perez, E., Bonifazi, P., Ruaro, M.E., Torre, V. (2007) On the dynamics of the spontaneous activity in neuronal networks. *PLoS ONE,* **2(5),** e439.

Mienville, J.M., Pesold, C. (1999) Low resting potential and postnatal upregulation of NMDA receptors may cause Cajal-Retzius cell death. *J. Neurosci.*, **19,** 1636-1646.

Morland, A.B., Baseler, H.A., Hoffmann, M.B., Sharpe, L.T., Wandell, B.A. (2001) Abnormal retinotopic representations in human visual cortex revealed by fMRI. *Acta Psychol (Amst),* **107,** 229-247.

Morland, A.B., Hoffmann, M.B., Neveu, M., and Holder, G.E. (2002). Abnormal visual projection in a human albino studied with functional magnetic resonance imaging and visual evoked potentials. *J Neurol Neurosurg Psychiatry* **72,** 523–526.

Owens, D.F., Boyce, L.H., Davis, M.B.E., and Kriegstein A.R. (1996) Excitatory GABA responses in embryonic and neonatal cortical slices demonstrated by gramicidin perforated-patch recordings and calcium imaging. *J Neurosci* **16,** 6414–6423.

Owens, D.F., Kriegstein, A.R. (2003) Is there more to GABA than synaptic inhibition? *Nat. Rev. Neurosci*, **3,** 715–727.

Oyster, C.W., Takahashi, E., Collewijn, H. (1972) Direction-selective retinal ganglion cells and control of optokinetic nystagmus in the rabbit. *Vision Res*., **12,** 183-193.

Paxinos, G., Watson, C., Pennisi, M., Topple, A. (1985) Bregma, lambda and the interaural midpoint in stereotaxic surgery with rats of different sex, strain and weight. *J. Neurosci. Methods*., **13,** 139-143.

Payne, J.A., Rivera, C., Voipio, J., Kaila, K. (2003) Cation–chloride co-transporters in neuronal communication, development and trauma. *Trends Neurosci.* **26,** 199-206.

Plotkin, M.D., Snyder, E.Y., Hebert, S.C., Delpire, E. (1997) Expression of the Na-K-2Cl cotransporter is developmentally regulated in postnatal rat brains: a possible mechanism underlying GABA's excitatory role in immature brain. *J Neurobiol*, **33(6),** 781-95.

Rivera, C., Voipio, J., Kaila, K. (2005) Two developmental switches in GABAergic signalling: the K+-Cl- cotransporter KCC2 and carbonic anhydrase CAVII. *J Physiol*, **562(Pt 1),** 27-36.

Rivera, C., Voipio, J., Payne, J.A., Ruusuvuori, E., Lahtinen, H., Lamsa, K., Pirvola, U., Saarma, M., Kaila, K. (1999) The K+/Cl– co-transporter KCC2 renders GABA hyperpolarizing during neuronal maturation. *Nature* **397,** 251–255.

Romero, M.F., Henry, D., Nelson, S., Harte, P.J., Dillon, A.K., Sciortino, C.M. (2000) Cloning and characterization of a Na+-driven anion exchanger (NDAE1). A new bicarbonate transporter. *J Biol Chem*, **275(32),** 24552-9.

Rosenberg, A.F., Ariel, M. (1991) Electrophysiological evidence for a direct projection of direction-selective retinal ganglion cells to the turtle's accessory optic system. *J. Neurophysiol*., **65,** 1022-1033.

Schmitz, B., Kasmann-Kellner, B., Schafer, T., Krick, C.M., Gron, G., Backens, M., and Reith, W. (2004). Monocular Visual Activation Patterns in Albinism as Revealed by Functional Magnetic Resonance Imaging. *Hum Brain Mapp.* **23,** 40 –52.

Schmolesky, M.T., Wang, Y, Creel, D.J., Leventhal, A.G. (2000). Abnormal retinotopic organization of the dorsal lateral geniculate nucleus of the tyrosinase-negative albino cat. *J Comp Neurol.* **427(2),** 209-19.

Schomberg, S.L., Bauer, J., Kintner, D.B., Su, G., Flemmer, A., Forbush, B., Sun, D. (2003) Cross talk between the GABA(A) receptor and the Na-

K-Cl cotransporter is mediated by intracellular Cl-. *J Neurophysiol.* **89,** 159-67.

Schomberg, S.L., Su, G., Haworth, R.A., Sun, D. (2001) Stimulation of Na-K-2Cl cotransporter in neurons by activation of Non-NMDA ionotropic receptor and group-I mGluRs. *J Neurophysiol.* **85,** 2563-75.

Schoppmann, A. (1985) Functional and developmental analysis of visual corticopretectal pathway in the cat: a neuroanatomical and electrophysiological study. *Exp. Brain Res.*, **60,** 363-374.

Shatz, C. (1977). A comparison of visual pathways in Boston and Midwestern Siamese cats. *J Comp Neurol.* **171(2),** 205-28.

St. John, R., and Timney, B. (1981). Sensitivity deficits consistent with aberrant crossed visual pathways in human albinos. *Invest Ophthalmol Vis Sci.* **21(6),** 873-7.

Staley, K., Smith, R. (2001) A new form of feedback at the GABA(A) receptor. *Nat Neurosci.* **4,** 674-6.

Staley, K.J., Proctor, W.R. (1999) Modulation of mammalian dendritic GABA(A) receptor function by the kinetics of Cl^- and HCO^-_3 transport. *J Physiol (Lond)* **519,** 693–712.

Stein, V., Nicoll, R.A. (2003) GABA generates excitement. *Neuron*, **37(3),** 375-8.

Sun, D., Murali, S.G. (1999) Na^{+}-K^{+}-$2Cl^{2+}$ cotransporter in immature cortical neurons: a role in intracellular Cl^{-} regulation. *J Neurophysiol* **81,** 1939–1948.

Sung, K.W., Kirby, M., McDonald M.P., Lovinger, D.M., Delpire, E. (2000) Abnormal GABAA receptor-mediated currents in dorsal root ganglion neurons isolated from Na-K-2Cl cotransporter null mice. *J Neurosci*, **20(20),** 7531-8.

Taylor, W.R., He, S., Levick, W.R., Vaney, D.I. (2000) Dendritic computation of direction selectivity by retinal ganglion cells. *Science*, **289,** 2347-2350.

Thiele, A., Distler, C., Korbmacher, H., Hoffmann, K.P. (2004) Contribution of inhibitory mechanisms to direction selectivity and response normalisation in macaque area MT. *Proc. Natl. Acad. Sci. USA*, **101(26),** 9810-5.

Torok, B. (2001). Albinism: diagnosis by visual evoked potentials. *Klin Monatsbl Augenheilkd.* 218(5), 327-31.

Vardi, N., Zhang, L.L., Payne, J.A., Sterling, P. (2000) Evidence that different cation chloride cotransporters in retinal neurons allow opposite responses to GABA. *J Neurosci.* **20(20),** 7657-63.

Wang, L., Kitai, S.T., Xiang, Z. (2006) Activity-dependent bidirectional modification of inhibitory synaptic transmission in rat subthalamic neurons. *J Neurosci*, **26(28),** 7321-7.

Yamada, J., Okabe, A., Toyoda, H., Kilb, W., Luhmann, H.J., Fukuda, A. (2004) Cl- uptake promoting depolarizing GABA actions in immature rat neocortical neurons is mediated by NKCC1. *J. Physiol.*, **557,** 829-41.

Zhu, L., Lovinger, D., Delpire, E. (2005) Cortical neurons lacking KCC2 expression show impaired regulation of intracellular chloride. *J Neurophysiol*, **93(3),** 1557-68.

ACKNOWLEDGMENTS

I take this opportunity to thank all those who have contributed to my thesis.

First of all, I would like to thank my thesis advisor Prof. Dr. KP Hoffmann for giving me the opportunity to perform this work in the Department of General Zoology & Neurobiology. I would also like to thank PD Dr. Georg Zoidl for gracefully agreeing to be my 2nd supervisor. Offers of assistance from Prof. Dr. Maxim Volgushev were also appreciated.

I gratefully acknowledge International Graduate School of Neuroscience (IGSN) for the financial support.

My years as a PhD student were much more pleasant due to the kind assistance of Evelyn Shutte, Catherine Botheroyd and Ursula Heiler.

Curriculum vitae

DMITRY DIYKOV

Tel: 0160 91910667

e-mail: dmitry_diikov@yahoo.com

PERSONAL DATA

Birth date:	June, 29, 1981
Birthplace:	Petrozavodsk, Karelia, 185014, Russia
Nationality:	Russian
Marital status:	Unmarried
Sex:	male

Education

Ph.D., Neuroscience, International Graduate School of Neuroscience, Ruhr University Bochum, Germany

Degree expected February 2008

Dissertation: Changes in GABAergic mechanisms and cation-chloride co-transport in albino visual cortex

Funding: International Graduate School of Neuroscience Scholarship

Supervisor: Prof. Dr. Klaus-Peter Hoffmann

MSc., Economical Geography, KSPU, Russia, June 2003

Thesis: A factor analysis of the interrelationship between social and technological variables and per capita gross national product

BSc., Natural Science, KSPU, Russia, June 2002

Employment

Junior Researcher

11.2003-2005

Sechenov Institute of Evolutionary Physiology and Biochemistry, Russian Academy of Sciences, Laboratory of Evolution of Neuronal Interactions, St. Petersburg, Russia

Responsibilities: Carrying out project titled “Investigation of neurosteroid modulation of GABA(A) receptors action in lamprey spinal cord neurons”.

Head of tourism department

04.2003-10.2003

“Nordic Travel”,

13 Kluchevskoe Shosse Street, Petrozavodsk, Karelia Russian Federation 185005

web: http://www.nordictravel.ru/

Publications

Diykov Dmitry, Barmashenko Gleb and Hoffmann Klaus-Peter. Development of chloride homeostasis in albino and pigmented rat visual cortex neurons. Submitted.

Dmitry Diykov, Andrey Turchinovich, Georg Zoidl, Klaus-Peter Hoffmann. Elevated intracellular chloride level in albino rat visual cortex neurons is mediated by Na-K-Cl co-transporter. Under submission.

Dmitry Diykov, Gleb Barmashenko and Klaus-Peter Hoffmann. Changes in E_{GABA} in visual cortex of pigmented and albino rats after metabotropic glutamate receptors block. In preparation.